We'd like to thank both referees for their comments, which have helped us to improve the manuscript. Next to all changes to the manuscript as a response to the remarks of the reviewers, which are all listed below, we have also made the following adjustments to the paper:

- We found a bug in our code, which caused an underestimation of the GIA correction that was applied to the GRACE observations, which led to bias mass changes. We have resolved this bug and updated all results accordingly. The updated results do not significantly alter any of the conclusions from this paper.
- We have updated the glacier mass balance dataset that was used to separate glacier mass changes from terrestrial water storage changes to a more recent version from Zemp et al. (2019).

Please find below a point-to-point response to all remarks from both referees. The referee comments are in black, our response is in blue, and updated manuscript text is in orange.

On behalf of all authors,
Thomas Frederikse

**Referee 1**

Summary: The manuscript presents an original approach to estimate trends in vertical land motions (VLM) and relative sea levels (RSL) due to the present-day mass redistribution (PDMR) occurring during the GRACE (Gravity Recovery And Climate Experiment) satellite mission (March 2002 – June 2017). PDMR changes are evaluated using the JPL (Jet Propulsion laboratory) GRACE mascon solutions [Watkins et al., 2015] and separated into a cryospheric and terrestrial water storage components, depending on the geographical location of mascons. This analysis is completed with an estimation of VLM and RSL trends due to Glacial Isostatic Adjustement (GIA), using the ensemble of GIA models from Caron et al. [2018]. The predicted VLM trends due to changes in the cryosphere, TWS and GIA are then compared to observations, using a subset of the GNSS data from the University of Nevada [Blewitt et al., 2018] matching the GRACE observation period. Finally, the authors discuss the impact of different VLM corrections on secular sea level rise averaged using a subset of 13 long tide gauge records.

**Major comment**
The manuscript provides a robust analysis of RSL and VLM trends due present-day ice melting, terrestrial water storage changes and glacial isostatic adjustment during the GRACE era. The link towards longer time scales is however not convincing. The major issue associated with the extrapolation of VLM corrections on secular time-scales is that we only have a very limited observation window (Figure 4, p7) and strongly non-linear processes. The problem is well stated by the authors (e.g. L10-12 p1), but, for several reasons, I doubt that their approach is appropriate to answer the issue, as it is claimed throughout the manuscript (e.g. L13-16 p1, L32-34 p2, L1-2 p16, L30-34 p17).

(i) VLM observations are decomposed in a cryosphere, TWS, GIA and residual components (eq. 3 p7), which except for GIA (and even this is arguable), all mix linear and non-linear processes. Therefore, non-linear processes in the residual VLM, due to local groundwater depletion, seismic deformation or other processes (e.g. L23-24 p2), are still present in the VLM correction and will generate a bias when extrapolated at longer time-scales.
We fully agree with the reviewer that our method does not fully solve the problem of non-linear processes when extrapolating the results. Our line of reasoning in this regard has been the following: the current state-of-the-art processing is just to extrapolate the trend derived from short GPS records along the whole tide-gauge record (e.g. Wöppelmann et al. 2014, Dangendorf et al. 2017), which has two limitations:

1. Vertical land motion derived over the short GNSS record is not per se representative for the long-term VLM signal.

2 When removing the VLM signal from tide-gauge records, we obtain geocentric sea level. As a result, sea-level reconstructions based on these records reconstruct global-mean geocentric sea level, which underestimates global-mean sea level because deformation of the sea floor is disregarded.

With our proposed method we remove one process that causes problem 1, while we also reduce the impact of problem 2. The reviewer is indeed right that there are many more processes that cause problem 1, which include processes we don't model (earthquakes, local subsidence from groundwater extraction etc.), and processes we do model, but with a sparse resolution inherent from the GRACE data, which could also cause unmodeled signals related to GIA and PDMD that are retained in the signals.

In the introduction, we added the following description to describe our line of reasoning, while again warning that we do not remove other processes from the GNSS data:
P1L30: In this paper, we propose an alternative approach to correct tide gauges for VLM: instead of removing the trend in observed VLM from GNSS records, the SED resulting from contemporary mass redistribution can be removed from the GNSS time series before computing the VLM trends that are used to correct tide gauges. With this method, we retain all other processes that cause local VLM, but we avoid that decadal and multi-decadal variability from contemporary mass redistribution aliases into VLM trends estimated from short GNSS records.

While not arguing that we fully solve the problem of VLM non-linearities, given the large impact of solid-earth deformation from contemporary mass redistribution, we do argue that the method we bring forward here is an improvement over the current practice of extrapolating the GNSS trends over the tide-gauge era. However, we sincerely want to avoid the unjustified impression that this work solves all problems with non-linearities in vertical land motion. Therefore, we have re-written parts of the abstract, introduction, methods, and conclusions to ensure that we do not 'oversell' this method.

In the abstract and introduction we now explicitly state that we only deal with solid-earth deformation due to GIA and contemporary mass redistribution, and we have added an explicit warning in the methods section:
P4L3: The term $R_{residual}(t)$ still contains all VLM that results from other processes. Many of these processes act on centennial time scales, such as sediment isostatic loading, compaction, and low-frequency tectonic processes. However, many other processes that act on shorter time scales, including groundwater depletion, hydrocarbon extraction, and co-seismic deformation, are also still present in the data. Therefore, extrapolating the trend in $R_{residual}(t)$ does avoid the bias due to contemporary mass redistribution, but not due to any other process that shows interannual and decadal variability, which means that the trend in $R_{residual}(t)$ does not represent the definite secular background trend.

In the conclusions we repeat this warning:
P19L30 Another important limitation is that we only consider the effects of solid-earth deformation due to GIA and contemporary mass redistribution, while many other local and large-scale processes, such as tectonics and local subsidence due to groundwater and hydrocarbon extraction, are still present in the residual VLM time series. Like SED, many of these processes are also highly non-linear, and therefore also cause problems when records are extrapolated. Therefore, the linear trend in residual VLM that we have computed cannot be regarded as the secular background trend that is free from any bias when extrapolated back in time. A full understanding of these processes is key to fully understand the impact of vertical land motion on tide-gauge observations. We hope that the method presented here will serve as a base for future studies to further separate the observed VLM trends into individual components by integrating new models of physical processes.

(ii) PDMR observations cannot fully account for the non-linear processes related to the cryosphere and TWS, given the limited time-span and spatial resolution of GRACE observations. These unmodelled processes will also end up in the residual VLM, be extrapolated at secular time-scales, and bias the correction applied to tide gauge observations.

The GRACE data indeed has a limited spatial and temporal resolution. We avoid the bias in residual VLM due to the limited time span by only using GNSS data that overlaps with GRACE, which is shown in Figure 5. We have re-visited the sections that discuss the limitations on the spatial resolution and the effects of local solid-earth properties in the conclusions section:
P19L23 Due to the coarse spatial resolution of the GRACE data, sharp gradients in mass redistribution are smeared out over larger areas. Since SED is sensitive to these local mass changes, the corrections computed here may under-estimate local SED in regions with strong spatial gradients. This issue could be one of the reasons of the un-explained residual land motion around Greenland, Antarctica, and Alaska visible in Figure 11. Another limitation is that we compute SED with an elastic model that assumes a laterally uniform Earth structure. In some regions, such as West-Antarctica, elastic properties can deviate from their global-mean values and visco-elastic effects could occur on decadal time scales, which leads to additional deformation on top of the elastic response (e.g. Hay et al., 2017).

(iii) The authors have tested their approach on a very limited subset of tide gauges, comprising only 13 sites. It is difficult to believe that this sample is statistically significant. RSL changes arise due to a complex mix of processes, that can be easily aliased with linear or non-linear VLM on such a small subset. The PSMSL database comprise many tide-gauge records that are significantly longer than VLM observations (with at least 370 tide gauges with more than 50 years of observations), that can be used to test the validity of VLM corrections. Besides, given that the main issue here is the extrapolation of non-linear processes in time, it would be good to show the impact of these corrections in a time-series analysis. Sole the mean and standard deviation of RSL trends are provided here, which is insufficient to assess the temporal and spatial variability expected from tide gauge measurements. Further analysis is therefore required to validate the assumption of the authors (i.e. their approach allows to get rid of the bias when extrapolating a VLM correction, based on the analysis of GNSS data, on secular time-scales). The paper could be limited to the analysis of recent (March 2002 – June 2017) mass exchanges between the continents and the oceans and their impacts on barystatic sea level changes, vertical land motions and relative sea level changes. The results would have to be put in context (the tool developed is not adapted to solve the issue brought forward here) and bring some clarifications on the following points.
We are afraid that we did not accurately describe the purpose of the application of our method to the long tide-gauge records, which is indeed not an appropriate validation of our method due to the low number of records. We have added this section, because is serves as an example to show that vertical land motion and contemporary mass redistribution have a large impact on trends estimated at tide-gauge locations.

The reason why we chose these tide gauges is that the discrepancy found by T16 is that this paper has shown a discrepancy between global sea-level reconstructions and long tide gauges. While it generated quite some attention in the sea-level community, the discrepancy has not yet been solved. In this example, we show that our proposed method could explain a part of this discrepancy.

We have added extra remarks to explicitly warn that this subset of tide gauges should not be seen as a validation of our method, but merely as a possible explanation of the T16 discrepancy:
P3L5: As an example of the effect of SED on VLM-corrected tide-gauge records, we revisit the analysis of Thompson et al. (2016, T16), who showed that the 20th-century sea-level trends observed at a set of long high-quality tide-gauge records could not be reconciled with the global-mean sea-level trends from recent reconstructions. We apply the residual VLM trends to the long tide-gauge records to see whether land motion could explain a part of this discrepancy.

A question that indeed remains open, is to which extent this new method affects other tide gauges. The major reason why we do not analyze all tide-gauge records in the PSMSL database is mainly because pairing tide gauges with GNSS stations is a non-trivial task, and it generally comes down to manually pairing GNSS stations with tide gauges. We'd argue that this task falls outside the scope of this paper. We have added a warning to the conclusions that the results from this subset should not be generalized to other tide gauges or global reconstructions:

P19L13: Note that we have only applied our method to a limited subset of tide gauges, which means that the reduction in local sea-level trends and the spread among stations is not necessarily representative for other tide gauges. Whether correcting tide gauges using our method affects global sea-level reconstructions is therefore still an unanswered question.

**Other comments and questions:**

General comment on methodological aspects: The "Data and methods" section is rather difficult to read. It would help to have a small paragraph and/or flowchart giving an overview of the method, that would link the various observational datasets and modelling approaches that are used together. The equation 3 at p7 is quite helpful to understand the author's approach but should come sooner in the paper.
We agree with the reviewer that the methodology section is not really clear. Reviewer 2 also brought this forward. Therefore, we have rewritten the methods section, and we have added a flowchart of the followed procedure as an extra figure, which hopefully helps in understanding and reproducing our results. The equations that describe our definition of 'Residual VLM' are now located at the beginning of the methods section.

*Section 2.1 GIA model*

p3: Is the ensemble of GIA predictions extracted from Caron et al [2018] only applied as an a-posteriori correction to the GRACE mascons solutions? Please, confirm or correct in the manuscript.
Yes, we use the ensemble to correct the GRACE mascon solution for GIA after restoring the original GIA correction applied to these mascons, but we also use the GIA ensemble to directly derive the GIA-related solid-earth deformation at the GPS locations. The new flowchart figure and the updated methods section now mention this procedure.

*Section 2.2 GRACE etc.*

p5 L3-4: "Each . . . mascon" How? What noise model is used? (+ typo in measurement)
We use the uncertainty estimates that come with the JPL mascon product, which are based on the error covariance matrix of the solution. Since the mass change estimates of in each mascon are more or less independent from its neighbors and other time steps, we assume that these errors are uncorrelated between time steps and mascons. The noise model is therefore 'white'. We have added an explanation to this section to clarify this.

p5 L6: "The uncertainty in the trend is dominated by GIA uncertainty": What are the other sources of uncertainty and how are they estimated?
We consider uncertainties in the measurement and in the GIA model, see also the answer to the previous remark. We have added a remark to clarify this.

p5 L19-21: Can you clarify how the separation between the cryosphere and TWS is done in mixed mascons?
Yes, for these mascons that contain glaciers, but which are not dominated by glaciers, we do the following: We use the in-situ observations from Zemp et al. (2019) to estimate the glacier mass loss in these mascons. Then, we can compute the TWS mass loss by subtracting the in-situ glacier mass loss from the total mass change in the mascon, as observed by GRACE. The in-situ mass changes from Zemp et al. (2019) come with an uncertainty. To propagate this uncertainty into the final estimates, we perturb each ensemble member based on this uncertainty. There was a short note on this in Paragraph 2.2, but we have extended the explanation to avoid any confusion.

*Section 2.3: Solid earth deformation etc.*

p6“we solve the SLE using the pseudo-spectral approach (Tamiesia, 2010)”: If I’m correct, this requires to express the load in spherical harmonics. How was this done? At which order? Please, also precise what load model is used (GRACE-derived PDMR mascons?)
Yes, that is indeed correct. The pseudo-spectral approach requires multiple synthesis and analysis steps between spherical and spherical harmonic coordinates, which we do up to degree and order 180 using the shtns library (Schaeffer et al. 2013). The input load is indeed the GRACE-derived PDMR mascon solution. We subsequently solve the sea-level equation for each ensemble member. We have revised the explanation to make this procedure clear.

*Section 2.4: GNSS etc*

p7 L7-9: This stresses the issue of the record length, which is too short to account for non-linear changes in VLM, and extrapolate them on longer time-scales.
Yes, we fully agree. As discussed before, this problem is one of the main reasons to write this paper. We have changed the introduction section to highlight this.

p8 L2-6: “Using the trend in zresidual (t) . . . from the record”: I do not understand the logic here. Once again, z residual is not supposed to be linear in any way, it is probably the largest source of error in the extrapolation of VLM correction at longer time-scales.
We are indeed far from sure (up to the point that we are quite sure of the opposite) that the residual VLM term is linear and can be safely extrapolated. However, with this procedure, we have at least removed one term that is not linear from the VLM data. See also our response above.

*Section 3: Results*

p8 last line: How do you explain a net land mass gain in TWS? You do mention later in the conclusion (p16 L20-22) that the global sea level rise due to PDMR (1.58 mm/yr Table 1) disagree with other estimates, that are usually higher. Why is the cryosphere contribution smaller with your approach? p 11 L6-7: Can you quantify the acceleration terms in ice mass loss? Is it comparable with other estimates?
During the revision process, we found a bug in the GIA correction that we applied to the GRACE data. We have resolved this bug, and as a result, the net land mass gain in TWS is not significant anymore, and the mass change estimates that we find are in line with most other estimates. We have updated the text, tables, and figures to reflect this. Furthermore, as explained above, we have decided to remove the discussion about our mass trends from the conclusions, as computing barystatic trends is not the main purpose of this paper. Although quantifying the acceleration in all these terms would be a very interesting study, we have decided not to include it in this manuscript for the following two reasons:

1. We want to limit the scope of this paper on how solid-earth deformation as derived by GRACE observations affect VLM at GNSS and tide-gauge locations. For this purpose, we have to come up with mass change estimates, but updating mass change estimates from glaciers, ice sheets and TWS from GRACE is not the primary goal of this paper. While the discussion on the mass changes already dilutes the discussion a bit, adding an extra discussion on the acceleration would weaken the focus of the paper even more.
2. Because the GIA correction that we apply is linear over the GRACE era, the uncertainty in the acceleration due to GIA is zero, while the acceleration uncertainty is likely primarily driven by decadal and multidecadal variations that will manifest as accelerations over the short data record. We do not analyze the temporal autocorrelation structure of our time series, and doing so in a proper way would be a study on its own. As a result, when we would quantify the uncertainty in the acceleration using the present approach, we’d get a very small uncertainty in the acceleration, and the resulting accelerations could easily be mis-interpreted.

Since our barystatic estimates are not to be considered as an update of previous estimates, many of which contain an in-depth analysis and tailor-made methodology to obtain individual mass changes, which is something we did not do. Therefore, we have removed the barystatic results from the abstract and the

conclusions section. As a final note, we'd like to emphasize that the underlying data is available from a repository, which means that everyone can compute the acceleration directly from the time series.

p 11 L20 : What is your indicator of "smooth temporal variations"?
This sentence is indeed not clear: what we meant was that the interannual variability in glacier and ice mass loss is small compared to the trend, and that therefore, the impact of the specific time span of the GNSS record has a limited effect on the deformation trend. We have rewritten the section to make this clear:
P13L13: The cryosphere-driven SED trends mostly show smooth spatial variations, and compared to the trend, the interannual variations are small, which implies that the specific time span of the GNSS record has a limited impact on the observed deformation rate.

p 13 L9 : Because GRACE resolution and mascon geometry is not adapted near the coast? Following that train of thought, it is unlikely that GRACE-derived TWS changes can account for the strong local variability evidenced at tide gauges.
We tried to explain a different process here that is not related to the mascon solution, but to the fact that mass changes occur on land, and the largest SED is therefore also expected to be in the middle of the region where the mass changes take place. Since tide gauges are located along the coast, they are generally not in the middle of the area where the mass change takes place (except maybe in cryosphere regions with marine-terminating glaciers), and the SED trends along the coast are thus expected to be smaller than the SED trends inland. Since we do not quantify this effect, we have removed this statement.

p 14 L10: this can easily be estimated with the application of a spatial filter on the observations (e.g. Pfeffer et al., 2017).
For some regions, especially in densely-sampled regions, such a filter would indeed provide a good estimate of long-wavelength features. However, in the regions that we refer to in this paragraph, this method comes with a problem, which is especially visible in Greenland. Here, virtually all GNSS stations are located along the coastline, which is also the region where the mass loss takes place, and the GNSS records all observe signals that are dominated by local processes, and are not representative for larger-scale processes. Applying a spatial filter here would just average the localized signals that are not representative for the whole region, and the resulting filtered mean would not be representative for the whole area. Therefore, we have decided not to implement such a filter.

p 14 L15 to 18: can you provide some quantitative information about the agreement/ disagreement between VLM observations and predictions (root mean square error, coefficient of determination, bias, maximum differences, distribution of the differences etc.)
We have added an overview of the aggregated statistics of the agreement between the model and observations to the results section.
P16L4: The mean linear trend for all 8166 stations is 0.34 mm $yr^{-1}$ with a standard deviation of 4.46 mm $yr^{-1}$, while the mean residual trend is 0.44 mm $yr^{-1}$ with a standard deviation of 4.28 mm $yr^{-1}$. The coefficient of determination (R2) of the modelled trends is just 7.5 percent. The full list of stations also contains many stations for which the MIDAS estimates very large uncertainties, sometimes exceeding 10 mm $yr^{-1}$. If we limit our station selection to those stations for which the uncertainty in the observed VLM trend is smaller than 1 mm $yr^{-1}$, which is the case for 4252 out of 8166 stations, we obtain a coefficient of determination of 34 percent and a reduction of the standard deviation from 2.30 to 1.86 mm $yr^{-1}$.

An interesting finding is that the model does not explain a large fraction of the observed trends, which changes when the trends with large standard errors are discounted. We added a remark about this in the conclusions section:
P18L28: This solid-earth deformation resulting from GIA and contemporary mass redistribution explains a substantial part of the observed GNSS trends: for all 8166 stations, we obtain a coefficient of determination of 7.5 percent. When we only consider stations for which the standard error in the observed VLM trend is smaller than 1 mm $yr^{-1}$, the coefficient of determination becomes 34 percent. This difference suggests that a non-

negligible part of the residual VLM trends can be attributed to the uncertainty in the estimated linear trends in VLM from noisy GNSS data, and that the uncertainties should not be overlooked when applying the observed and residual VLM trends to tide-gauge data.

p14 L20: why do you limit your analysis to these 15 stations? why such a restrictive selection?
Please see our response to the major point iii above on why we chose this approach.

p15 L7 to 8 "For the full model . . . GIA RSL trend" Why? How does that help with the extrapolation of non-linear processes in time?
It actually avoids the extrapolation of a non-linear process in time, as a non-linear process has been removed from the VLM observations. We have added an explanation about this:
P17L10: The 'full' model removes the spatial variations due to GIA and local VLM not related to SED, while it avoids the extrapolation of the non-linear SED signal due to contemporary mass redistribution. In the 'full' model, sea-floor deformation signals due to contemporary mass redistribution and GIA are also retained in tide-gauge records.

p 15 L10 "assuming a power law spectrum" to describe temporally correlated noise?
Yes, we have added a clarification to the text.

p 15 L11: Why do you choose the T16 subsample? How does it help to validate your approach?
Please see our response to the major point iii above on why we chose this approach.

p 16 L1-2: How are these issues resolved?
This sentence was not completely clear: we only resolve the problems due to contemporary mass redistribution. We have changed the sentence to reflect this.

p16 L9: Yes, the "sampling bias" is a huge problem that needs to be addressed. More observations are available to start with.
This sampling bias actually refers to T16 who argue that 20$^{th}$-century sea-level rise is likely larger than the average at the 15 tide-gauge stations due to sea-level fingerprints and ocean dynamics. We put this sentence here, because the argumentation in T16 can be roughly summarized as follows: 1. The trend at long TG records is larger than some recent GMSL reconstructions. 2. Due to their location, we expect these tide gauges to underestimate rather than overestimate the 20$^{th}$-century GMSL trend. Therefore, these observations cannot be reconciled with recent reconstructions. Here, we show that vertical land motion can explain step 1, but we do not look into step 2 here, so the discrepancy is not yet fully solved. We have changed the sentence to clarify this.

*Section 4: Conclusion*

p 16 L20: Why this disagreement? This should be discussed earlier in the manuscript.
As described above, we found a bug in our code that led to land-mass changes that were too small. After correcting this bug, the discrepancy has become smaller, but still significant. A likely candidate for this discrepancy has been found in a recent paper from Uebbing et al. (2019), who found that some of these estimates have treated the global atmospheric correction (GAC) in an inconsistent way. However, since the main focus of this paper is about local SED effects rather than updating the global sea-level budget and its contributors, we have removed this discussion from the conclusions.

p 17 L6: How do you estimated uncertainties that are not related to GIA?
The uncertainties in the other terms are all derived from the ensemble. Since the estimates of contemporary mass redistribution depend on the GIA correction applied to the GRACE data, GIA uncertainty propagates into all other quantities. Together with the GRACE measurement uncertainty and the uncertainty in the estimated VLM trends from GNSS data, this results in uncertainties for all quantities. We have added Figure 1 which gives an overview on how the ensemble is used to derive all quantities and uncertainties.

p 17 L 23: please provide metrics to illustrate the agreement/disagreement between VLM observations and predictions.
We have added these metrics to the results section. See also our response to the comments above.

p 17 L 33: The authors did not convince me that their approach avoids the bias, due to the extrapolation of non-linear VLM. It does not logically follow their assumptions and has not been evidenced in the results. However, they provide insights on the mechanisms driving recent (GRACE era) sea level changes and solid earth deformation, which is, I think, useful results.
Please see our response to the general comments above.

**Details:**

*Abstract:*
L1 to 3: rephrase the first sentence to be more readable (less "and", please)
We have updated the abstract with shorter sentences, and we have rephrased this sentence as well.

L8: "the temporal variations affect GNSS-derived VLM": temporal variations of what?
This sentence has been replaced as well.

L13 to 16: This is very confusing. Separating VLM observations in GIA and PDMR components does not separate linear from non-linear components (see major comment).
We have re-phrased this sentence as well to emphasize that we only investigate the bias due to contemporary mass redistribution.

*Introduction:*

L32 to34: see major comment
Adjusted, see above

*Data and methods:*

L10: "GIA affects GRACE observations . . .": replace by causes changes in the gravitational potential observed by GRACE satellites or equivalent to keep the same structure for each proposition of the sentence.
Fixed

L27 p3: "we bin the quantity of interest": not sure what bin means
We have re-phrased this sentence:
P5L21: We can also derive an empirical PDF from the ensemble, from which confidence intervals at any level can be computed. To compute the empirical PDF, we first sort the values from low to high. Then we define 20 bins between the 1st and 99th percentile of these values and compute the sum of the likelihood of all ensemble members that fall within each bin. The number of 20 bins is chosen as a trade-off between resolution and sample size

eq 3: why using two different variables (R and z)?
We have replaced $z$ by $R$ throughout the text.

p 7 L14: use of the term "uplift": replace by vertical displacement of the earth's surface (or equivalent)?
This sentence has been re-phrased, and we have checked that now every occurrence of the word 'uplift' refers to land coming 'up'.

Results p10 L8 and 9: "considerable" means how much?

We have rephrased the sentence and removed ‘considerable’:
P11L21 Figure 8 shows that, next to uplift at locations where the ice-mass loss takes place, mass changes in the cryosphere result in some far-field SED signals, including subsidence of about 0.5 mm $yr^{-1}$ around Australia, and an uplift signal with a similar magnitude in Europe and Northern Asia.

Conclusion p16 L14- 17: please reformulate to clarify
We have re-ordered the conclusions, and this sentence is not there anymore.

Figures: It is difficult to read the color scales of figure 7, 8 (bottom row), 9 and 10. Is possible to provide a bit more contrast to have a better idea of the range of variations of RSL and VLM trends? Otherwise, provide numbers in the legend or in the text.
We have updated the color scales which should now have more contrast in these figures. Alternatively, all individual data is available from the data in the repository.

**Reviewer 2**

The paper aims to develop estimates for deformation due to GIA and present-day mass redistribution with uncertainty estimates. The deformation patterns are explained and used to correct tide-gauges. It is an original idea to address a highly relevant problem. It is shown that this correction improves consistency between sea-level trends from tide
gauges and sea level reconstructions, and offers potential for better regional sea level projections. I see no problems in the methodology. Therefore I recommend the paper to be published after addressing two main comments below, and the long list of textual comments connected to these.

Correcting tide gauges only holds for the time period of the data, or the time for which the model is valid, while one of the reasons for decomposing the relative sea level rate is to make projections outside the data range. The corrections are necessarily based on limited time span and also do not include regional deformation processes which can vary in time. This is an important limitation of the paper that is not discussed well in section 3.4 and in the conclusions, see specific comments below.

A second problem in the paper is the way it is written. Logic is sometimes hard to follow, procedures are not described clearly or are not explained, the use of words that should have a precise meaning is a bit sloppy (words such as trend or linear trend, deformation, model, relative sea level or just sea level). Several examples are given below. A thorough revision of the text is necessary because it now guessing is required from the reader in several places to put the pieces of the puzzle together.

A pdf is attached with small textual comments or typos.

**Specific comments**

The abstract is a mix of describing the processes and the methodology. I suggest to move the methodology to the last paragraph where the methodology is now partly described
Thanks for this suggestion, we have re-written parts of the abstract and we have removed some of the methodological details to improve the readability.

*Introduction*

The introduction is difficult to follow because it is a mix of a background and methodology, and the description of the objective is scattered. I suggest to reorder the introduction to more clearly separate background, problem statement, methodology and application separately. Also the first part of the conclusion and the introduction should be better aligned.
We have re-written the introduction, and now we start with a statement of the problems that occurs when long tide-gauge records are corrected for VLM using short GNSS records. We have also re-written parts of the conclusions to keep the focus on the effects of SED on VLM and sea-level observations.

Page 1
Suggest to add Wu and Peltier (1984) to Milne and Mitrovica (1998)
We have added the reference.

Page 2
- line 3 I get the impression that sea level and relative sea level are not used consistently according to their definitions, please check
We have checked and updated the paper, and now we use global-mean sea level, geocentric sea level and relative sea level throughout the paper.

- line 15 and further: use trend or linear trend consistently

Fixed

- line 34: “to avoid this possible bias” Please make clear what bias you refer to and what part you aim to remove. If the bias refers to the (local) processes in line 21 and further then correcting for PDMR and GIA alone is not sufficient. If this bias refers to the bias due to PDMR alone (line 28 and further) it is not clear why you would remove GIA as well. Also the time-period seems relevant because you can not use the computed PDMR induced deformation beyond the period of the data.
This point was also risen by the other reviewer. We have changed the text throughout the manuscript to make clear that we only look for the bias related to contemporary mass redistribution, while other processes could also have a similar effect.

*Page 3*

- Line 6: the text contains ‘estimates of GIA’, ‘GIA solutions’,’model ensemble’. Please make it more consistent.
Fixed

- Line 9: title of section 2.1 , I suggest to use something like ’prediction ensemble’ because you do not actually discuss the model
Fixed: changed to ‘GIA estimates’

- line 15: It seems to be partly circular reasoning when you use model ensembles scored according to fit to GNSS data to correct GNSS data. Please address this in the text.
That’s true. We have added a note about this:
P5L7: Note that some circular reasoning is introduced here, as we use the same GNSS data to determine residual VLM that was used to benchmark the GIA estimates. However, since the vast majority of the benchmark data comes from paleo indicators, and the cost function used to compute the likelihood is much more sensitive to paleo rather than GNSS data, the impact on this circular reasoning on the results is limited.

*Page 4*

- Line 5: please explain why ocean bottom pressure changes are not used, because they are a form of PDMR
We have done this because the spatial variations in bottom pressure are very small compared to land-mass changes. We have added a remark:
P5L31 We only look into mass changes on land, and do not take ocean-bottom pressure changes driven by ocean dynamics into account, since its spatial variations are much smaller than the land mass changes (e.g. Watkins et al, 2015).

- Line 6: please discuss the possible effect, if any, of this filter on the final estimates, as the main interest is in deformation along the coast.
This filter reduces the leakage of mass signals between land and ocean. Therefore, the spatial distribution of mass changes in coastal locations is improved by applying this filter. Note that this filter is part of the standard processing of JPL mascons. We have added a remark about the improved spatial representation:
P7L1: For mascons that contain a coastline, a Coastline Resolution Improvement (CRI) filter has been used to prevent the leakage of gravity signals between land and ocean, which leads to a better spatial representation of mass changes in coastal regions.

*Page 5*

Potential uncertainty from determining deformation due to ice sheets, glaciers and TWS should be addressed here.
We have added a note about this uncertainty to the conclusions:

P19L26: Another limitation is that we compute SED with an elastic model that assumes a laterally uniform Earth structure. In some regions, such as West-Antarctica, elastic properties can deviate from their global-mean values and visco-elastic effects could occur on decadal time scales, which leads to additional deformation on top of the elastic response.

*Page 6*

- Line 13: It is more useful to say what is neglected: viscous effects due to PDMR changes before and during the period of interested, and where these effects could occur
We have added a remark about this, see previous comment.

- Line 15: please add a reference as there has been discussion about the methodology
We have added a reference to Milne & Mitrovica (1988), which describes the methodology that we use to compute the rotational feedback.

*Page 7*

- Line 14: how is the height anomaly defined?
With respect to the mean height of the time series. However, since we are interested in height changes, the mean height itself does not affect our results. We have added a remark:
P3L26: We express height anomalies with respect to the mean height of each time series, but since we are interested in height changes, the mean height itself does not affect our results.

Section 2.4 It would help the reader if you explain what result you are after in this section before describing possible corrections.
We have re-ordered the methods section, and we now start with an overview of the residual VLM, as that is where we are after.

*Page 9*

- line 7-15: There are probably existing studies on TWS and land mass changes that these results can be compared too.
As far as we know, almost all studies that quantity TWS changes use GRACE, and not many studies exist that quantify TWS changes from models. A study by Scanlon et al (2018) discusses the problems that models have to estimate TWS changes. We add a discussion about this in the conclusions:
P19L21: While for ice mass changes model results show good agreements with observations, model estimates of terrestrial water storage changes are still less reliable than GRACE observations (Scanlon et al., 2018), which in turn limits the ability to use models to estimate SED.

*page 11*

section 3.2, the last paragraph in the section needs a conclusion, which could perhaps be moved here from section 3.3
We have rewritten the concluding remarks of this section.

- line 18: do you mean the solid earth deformation trend from section 3.2? How do GNSS observations play a role there?
Yes, we have re-phrased this expression.

- line 20: the temporal variations are not shown in figure 11
The word temporal was indeed not correct here. We have removed it.

*page 13*

- line 3: It should be explained what kind of cryosphere changes could cause these kind of uplifts

We have re-phrased these sentences:

P13L16: These trends do not only reflect the well-known near-field uplift signals at or near the ice-mass loss locations, which dominate the VLM signal for many regions where ice mass loss occurs, but also in the far field, with notable uplift in large parts of Europe and the US, and subsidence in Australia.

*page 14*

Line 2: discussion of the uncorrected trend could be moved before the statement that the observations will be corrected.

We re-shuffled this section, and now we start with discussing the observed VLM trends before moving to the corrections.

Line 8: "even considering the uncertainty." This is ambiguous. Please make clear whether you mean that the ensemble mean is stronger or not, or whether you talk about a statistically significant increase

We have removed the statement about the uncertainty, and made clear that we discuss the ensemble mean value here.

Line 20: "partially repeat the analysis". Describe the analysis because now it is not clear what you are doing different and why in what follows.

We have removed this sentence and we expanded the description of what we have actually done.

*Page 15*

Line 1: specify what you mean by "in the vicinity" From line 5 onwards the text is very hard to follow. You need to explain that the goal is and why certain choices are made. The only explanation is that the analysis of Thompson et al. (2016) is partially repeated. Please add intepretation of the figure to line 12, now it is left to the reader. Several comments and questions on this section can be found in the pdf.

We have expanded the explanation of this section to make it better understandable.

*Page 16*

Line 1: I don't agree that both issues are resolved (same for page 17 line 32). Regional deformation such as given in page 2 line 22 will also not follow a constant trend so you can not use GNSS data or models with a shorter period than the tide gauge period and expect that extrapolation of deformation models or data works fine, or am I missing something?

We agree that this conclusion is misleading: we only considered the effects of contemporary mass redistribution. We have changed the text throughout the manuscript to make sure that it is clear that any other non-linear process is still in the data.

Line 10: "the gap discussed by T16" specify which gap for readers that have not read that paper

We have added a clarification:

P18L14: Note that T16 also argues that averaging the linear trend in sea level from these long tide gauges likely underestimates the global-mean sea-level trend due to the spatial patterns associated with ice-mass loss and ocean dynamics. Here, we do not consider this spatial sampling bias, so the gap between the long tide-gauge records and global-mean sea-level reconstructions discussed by T16 cannot yet be fully reconciled from these results.

*Page 17*

Line 25: "uncertain GIA contribution" explain if this means that the uncertainty in the GIA models ensemble is underestimated

Yes, that is indeed what we wanted to stated. We have added a remark:

P19L3: A likely candidate for this residual trend is the uncertain GIA contribution: the global model that we use does not account for lateral variations in the mantle viscosity structure and is not optimized for a specific region,

and uncertainties in the deglaciation history that are not fully represented in the GIA ensemble could lead to an underestimation of the uncertainty in formerly glaciated regions.

Please also note the supplement to this comment
We have addressed all typos and unclear statements that were brought forward in the supplement.

**References**


Dangendorf, S., Marcos, M., Wöppelmann, G., Conrad, C. P., Frederikse, T., & Riva, R. (2017). Reassessment of 20th century global mean sea level rise. Proceedings of the National Academy of Sciences, 114(23), 5946–5951. https://doi.org/10.1073/pnas.1616007114

Hay, C. C., Lau, H. C. P., Gomez, N., Austermann, J., Powell, E., Mitrovica, J. X., … Wiens, D. A. (2017). Sea Level Fingerprints in a Region of Complex Earth Structure: The Case of WAIS. Journal of Climate, 30(6), 1881–1892. https://doi.org/10.1175/JCLI-D-16-0388.1

Milne, G. A., & Mitrovica, J. X. (1998). Postglacial sea-level change on a rotating Earth. Geophysical Journal International, 133(1), 1–19. https://doi.org/10.1046/j.1365-246X.1998.1331455.x

Scanlon, B. R., Zhang, Z., Save, H., Sun, A. Y., Müller Schmied, H., van Beek, L. P. H., … Bierkens, M. F. P. (2018). Global models underestimate large decadal declining and rising water storage trends relative to GRACE satellite data. Proceedings of the National Academy of Sciences, 115(6), E1080–E1089. https://doi.org/10.1073/pnas.1704665115

Schaeffer, N. (2013). Efficient spherical harmonic transforms aimed at pseudospectral numerical simulations. Geochemistry, Geophysics, Geosystems, 14(3), 751–758. https://doi.org/10.1002/ggge.20071

Thompson, P. R., Hamlington, B. D., Landerer, F. W., & Adhikari, S. (2016). Are long tide gauge records in the wrong place to measure global mean sea level rise? Geophysical Research Letters, 43(19), 10,403-10,411. https://doi.org/10.1002/2016GL070552

Uebbing, B., Kusche, J., Rietbroek, R., & Landerer, F. W. (2019). Processing choices affect ocean mass estimates from GRACE. Journal of Geophysical Research: Oceans. https://doi.org/10.1029/2018JC014341

Wöppelmann, G., Marcos, M., Santamaría-Gómez, A., Martín-Míguez, B., Bouin, M.-N., & Gravelle, M. (2014). Evidence for a differential sea level rise between hemispheres over the twentieth century. Geophysical Research Letters, 41(5), 1639–1643. https://doi.org/10.1002/2013GL059039

Watkins, M. M., Wiese, D. N., Yuan, D.-N., Boening, C., & Landerer, F. W. (2015). Improved methods for observing Earth's time variable mass distribution with GRACE using spherical cap mascons. Journal of Geophysical Research: Solid Earth, 120(4), 2648–2671. https://doi.org/10.1002/2014JB011547

Wu, P., & Peltier, W. R. (1984). Pleistocene deglaciation and the Earth's rotation: A new analysis. Geophysical Journal International, 76(3), 753–791. https://doi.org/10.1111/j.1365-246X.1984.tb01920.x

Zemp, M., Huss, M., Thibert, E., Eckert, N., McNabb, R., Huber, J., … Cogley, J. G. (2019). Global glacier mass changes and their contributions to sea-level rise from 1961 to 2016. Nature, 568(7752), 382–386. https://doi.org/10.1038/s41586-019-1071-0

# The imprints of contemporary mass redistribution on ~~regional~~ local sea level and vertical land motion observations

Thomas Frederikse[1], Felix W. Landerer[1], and Lambert Caron[1]

[1]Jet Propulsion Laboratory, California Institute of Technology, Pasadena, California, USA

**Correspondence:** Thomas Frederikse (thomas.frederikse@jpl.nasa.gov)

**Abstract.** ~~We derive trends and monthly anomalies in global and regional sea-level~~ Observations from permanent GNSS stations are commonly used to correct tide-gauge observations for vertical land motion (VLM). We combine GRACE observations and ~~solid-earth deformation that result from mass redistribution observed by GRACE and~~ an ensemble of ~~GIA models. With this ensemble, we do not only compute mean changes, but we also derive uncertainty estimates of all quantities. We find that over the GRACE era, the trend in land mass change has led to a~~ glacial isostatic adjustment (GIA) predictions to assess and evaluate the impact of solid-earth deformation (SED) due to contemporary mass redistribution and GIA on VLM trends derived from GNSS stations. This mass redistribution causes relative sea-level ~~trend of 1.28-1.82 mm yr$^{-1}$, which is driven by ice mass loss, while terrestrial water storage has increased over the GRACE period, causing a sea-level drop of 0.11-0.47 mm yr$^{-1}$. This redistribution of mass causes sea-level and deformation~~ (RSL) and SED patterns that do not only vary in space, but also ~~in time. The temporal variations affect GNSS-derived vertical land motion (VLM) observations, which are now commonly used to correct tide-gauge observations.~~ exhibits large inter-annual variability signals. We find that for many ~~GNSS~~ stations, including ~~GNSS~~ stations in coastal locations, ~~solid-earth deformation resulting from present-day mass redistribution causes trends in~~ this deformation causes VLM trends on the order of 1 mm yr$^{-1}$ or higher. ~~Since~~ In multiple regions, including the Amazon Basin and large parts of Australia, the SED trend flips sign between the first half and second half of the 15-year GRACE record. GNSS records often only span a few years, ~~these trends are generally not representative for the tide-gauge records , which often span multiple decades, and extrapolating them backwards in timecould cause substantial biases~~and due to these inter-annual variations, SED causes substantial biases when the linear trends in these short records are extrapolated back in time.

~~To avoid this possible bias , we computed trends and associated uncertainties for 8228 GNSS stations after removing deformation due to GIA and present-day mass redistribution.~~ We propose a new method to avoid this potential bias in VLM-corrected tide-gauge record: instead of correcting tide-gauge records for the observed VLM trend, we first remove the effects from GIA and contemporary mass redistributions from the VLM observations before computing the VLM trend. This procedure reduces the extrapolation bias induced by SED and it also avoids the bias due to sea-floor deformation: SED includes net sea floor deformation, which is ignored in global-mean sea-level reconstructions based on VLM-corrected tide-gauge data. We apply this method to 8166 GNSS stations. With this separation, we are able to explain a large fraction of the discrepancy between observed sea-level trends at multiple long tide-gauge records and the ~~reconstructed~~ global-mean sea-level trend from recent reconstructions.

## 1 Introduction

~~Mass loss from glaciers and ice sheets (?) and changes in terrestrial water storage (TWS, ?) have resulted in an increase of ocean mass and a rise of global sea level over the past decades (?). This redistribution of mass over the earth surface causes substantial changes in the earth's gravity field, the rotation parameters, and it deforms the solid earth (???). Due to these effects, mass redistribution results not only in global~~ Recent global and local studies have shown that local vertical land motion (VLM) explains a significant part of spatial variations in tide-gauge trends, which, if ignored, biases estimates of global and local sea-level changes ~~, but also in regional patterns of~~ (e.g. ???). Global and local sea-level ~~change and solid-earth deformation ('deformation' from here on). The regional relative~~ studies therefore often use GNSS records to correct tide-gauge records for VLM (???). Despite yielding significant improvements, such a correction does introduce two problems:

1. The resulting sea-level ~~(RSL) patterns are observed by tide gauges (e.g. ?), while deformation is observed by permanent GNSS stations as vertical land motion (VLM, ?). A thorough understanding of the causes of these regional patterns of sea level and VLM is an important prerequisite to projecting future regional~~ observations are essentially geocentric sea-level ~~changes (?) and to using local observations to infer global sea-level changes (??). The Gravity Recovery and Climate Experiment (GRACE, ?) satellite mission has provided estimates of present-day mass redistribution (PDMR) over the earth surface with unprecedented resolution and accuracy (?). The resulting regional RSL and deformation patterns can be directly computed from GRACE observations(?). In this paper, when we refer to 'RSL', we refer to RSL changes, not its mean value. Glacial isostatic adjustment (GIA) also cause regional RSL and deformation patterns, and to obtain PDMR changes from GRACE, its observations must be corrected for GIA. However,~~ (GSL) observations. Global and local reconstructions based on these corrected records reconstruct GSL changes. Since not only the sea surface, but also the sea floor can move vertically, global-mean GSL, which is blind to movements of the sea floor, deviates from the ~~effects of GIA come with an uncertainty (e.g. ?), which in turn affects GRACE estimates and the resulting global and regional RSL and deformation patterns. We use GRACE observations and the large ensemble of GIA solutions from ? to derive PDMR estimates and the resulting global and regional deformation and RSL changes. We also derive robust uncertainties of these estimates. We use these deformation estimates to derive VLM trends that are corrected for GIA and PDMR. VLM trends derived from GNSS time series are more and more often used to correct~~ total change in ocean volume. As a result, global-mean GSL reconstructions could be biased with respect to global-mean sea-level ~~observations from tide gauges for the impact of local VLM (????). This correction has led to improved estimates of global and regional sea-level changes (????). However, in most of these studies it~~ (GMSL) changes, which are defined as the total change in ocean volume, divided by the ocean area (???).

2. It is commonly assumed that the linear VLM trend, derived over the ~~short~~ length of the GNSS record, ~~is~~ which is typically a few years, is representative for the full time span of the associated tide gauge, which often covers multiple decades.

This assumption generally holds for VLM caused by glacial isostatic adjustment (GIA) outside low-viscosity regions (e.g. **?**), sediment isostatic adjustment, and compaction (**?**)~~, but for many processes,~~ . However, forprocesses such as subsidence due to local groundwater depletion (**??**) and co-seismic and post-seismic activity (**?**), this assumption does not hold. ~~As a result, correcting long tide-gauge records for the VLM trend observed~~ Therefore, the extrapolation of the derived linear VLM trend over the short GNSS ~~record could~~ time span over the long tide-gauge records can introduce a bias (**?**). ~~PDMR could also be a source of such a bias. Both ice mass loss and TWS changes cause substantial deformation trends (??), and these trends explain a~~

Contemporary mass redistribution contributes to both problems: when mass is moved over the Earth surface, the Earth deforms elastically as a response to these changes in the load (**?**). This solid-earth deformation (SED) translates into local VLM that is registered by GNSS stations. Mass loss from glaciers and ice sheets and changes in terrestrial water storage (TWS) have resulted in an increase of ocean mass and a rise of global-mean sea level over the past decades (**?**), but have also caused substantial local SED patterns (**??**). This process explains a non-negligible part of VLM signals observed by permanent GNSS stations ~~(??)~~(**???**). Due to the accelerating pace of ice-mass loss (**?**) and the large decadal and multi-decadal TWS variability (**???**), the resulting ~~deformation cannot be~~ SED is highly non-linear in time, and thus cannot be accurately described by a ~~linear trend on long time scales, and trends over the~~ single linear trend that holds on multiple temporal scales. Therefore, linear trends in SED over the shorter GNSS time span are in general not representative ~~for~~ of longer periods. Over the last few decades, contemporary mass redistribution has also driven global and local sea-floor deformation, resulting in a difference between GMSL and global-mean GSL changes on the order of 0.1 mm/yr over the last decades (**?**), with larger deviations on local scales(**?**).

~~To avoid this possible bias, we compute VLMtrends corrected for GIA and PDMR at a global network of 8,228 stations from the Nevada Geodetic Laboratory database (?). These VLM trends~~ In this paper, we propose an alternative approach to correct tide gauges for VLM: instead of removing the trend in observed VLM from GNSS records, the modelled SED resulting from contemporary mass redistribution can be subtracted from the GNSS time series before computing the VLM trends that are used to correct tide gauges. With this method, we retain all other processes that cause local VLM, but we avoid that decadal and multi-decadal variability from contemporary mass redistribution aliases into VLM trends estimated from short GNSS records. We estimate SED from the Gravity Recovery and Climate Experiment (GRACE, **?**) and a large ensemble of GIA estimates from **?**, C18 to derive contemporary mass redistribution estimates and the resulting SED and RSL changes with robust uncertainties. After subtracting this SED, the linear VLM trends and associated uncertainties can be used to correct tide-gauge observations~~for local VLM while avoiding the aforementioned possible bias. Furthermore, these trends can be used for any study that relies on VLM estimates, but for which deformation due to GIA and PDMR are unwanted signals. As an example application, we apply the corrected VLMtrends on a subset of the~~ , while reducing the impact of both aforementioned problems. As an example of the effect of SED on VLM-corrected tide-gauge ~~data set used in ?, T16. T16 find that many of the longest~~ records, we revisit the analysis of **?**, T16, who showed that the 20th-century sea-level trends observed at a set of long high-quality tide-gauge ~~records show higher~~ records can not be reconciled with the global-mean sea-level ~~trends for the 20th century than estimated by the recent global reconstructions from ? and ?. We show that correcting these long-term~~ trends from

recent reconstructions. We apply the residual VLM trends to the long tide-gauge ~~records for local VLMexplains a large part of this discrepancy.~~ records to see whether land motion explains a part of this discrepancy.

## 2 Data and methods

~~In this section, we~~ The local relative sea-level (RSL) and solid-earth SED patterns that result from GIA and contemporary mass redistribution are caused by the geoid, rotational, and deformation (GRD) response to changes in the load at the surface of the Earth (**????**). (RSL, $\eta$) changes are defined as a change of the sea surface relative to the underlying sea floor, while geocentric sea-level (GSL, $\zeta$) changes are change of the sea surface relative to the center of the Earth. These changes are related to geoid changes ($G$) and SED ($R$) according to:

$$\eta(\theta,\phi,t) = \mathcal{M}(t) + G(\theta,\phi,t) - R(\theta,\phi,t) \tag{1}$$

$$\zeta(\theta,\phi,t) = \mathcal{M}(t) + G(\theta,\phi,t) = \eta(\theta,\phi,t) + R(\theta,\phi,t). \tag{2}$$

$\theta$ and $\phi$ denote latitude and longitude, and $t$ time. The global-mean relative sea-level change due to water that enters or exits the ocean is called barystatic sea-level change. The globally-constant term $\mathcal{M}$ is needed to ensure that the barystatic sea-level change is equal to the total water volume entering or exiting the ocean, although $\mathcal{M}$ itself is not necessarily equal to the barystatic sea-level change. The difference between Equations 4 and 2 is the solid-earth deformation $R$, which means that when we subtract VLM from the tide-gauge observations, we obtain GSL changes. This equation also shows that global-mean GSL is not equal to barystatic sea-level change, since $R$ averaged over the global ocean is not necessarily equal to zero: the ocean can become deeper or shallower as a whole due to SED. VLM observations can be separated into three components: one related to GIA, one related to contemporary mass redistribution, and a residual VLM term:

$$R_{\text{obs}}(t) = R_{\text{GIA}}(t) + R_{\text{CMR}}(t) + R_{\text{residual}}(t). \tag{3}$$

$R_{\text{obs}}(t)$ is the height anomaly at time $t$ observed by GNSS. We express height anomalies with respect to the mean height of each time series, but since we are interested in height changes, the mean height itself does not affect our results. $R_{\text{GIA}}(t)$ and $R_{\text{CMR}}(t)$ are the height anomaly caused by GIA and contemporary mass redistribution. $R_{\text{residual}}(t)$ is the residual anomaly, which is the observed height anomaly that cannot be explained by GIA and contemporary mass redistribution. If we now correct our tide-gauge record with the linear trend in $R_{\text{residual}}(t)$ instead of the commonly-used trend in $R_{\text{obs}}(t)$, we do not remove the SED contribution from the tide-gauge record, while we do remove all unexplained local VLM. Therefore, we retain the effects of sea-floor deformation due to GIA and contemporary mass redistribution in the tide-gauge record, and we avoid that variations in $R_{\text{CMR}}(t)$ over the short GNSS record are extrapolated over the full tide-gauge record. The term $R_{\text{residual}}(t)$ still contains all VLM that results from other processes. Many of these processes act on centennial time scales, such as sediment isostatic loading, compaction, and low-frequency tectonic processes. However, many other processes that act on shorter time scales, including groundwater depletion, hydrocarbon extraction, and co-seismic deformation, are also still present in the data. Therefore, extrapolating the trend in $R_{\text{residual}}(t)$ does avoid the possible extrapolation bias due to contemporary mass

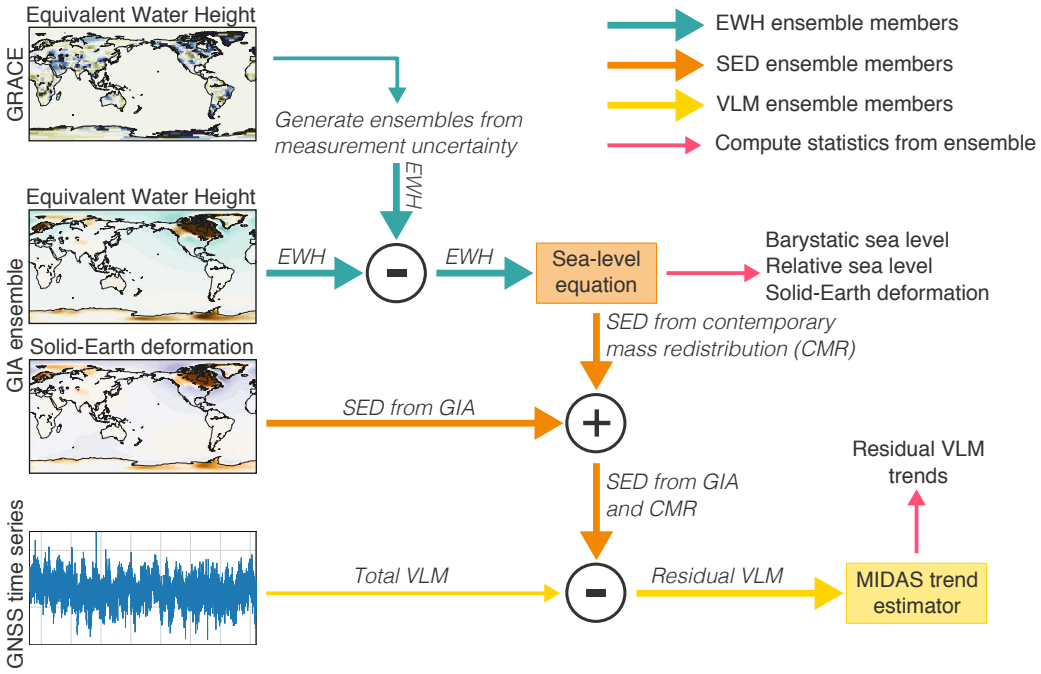


**Figure 1.** Overview of the processing steps taken to compute trends in residual VLM from the GRACE observations, GNSS time series, and GIA estimates. Thick arrows denote ensemble computations, while thin lines denote non-ensemble steps.

redistribution, but not due to any other process that shows inter-annual and decadal variability. This separation does not mean that the trend in $R_{\text{residual}}(t)$ can be considered to be the definite secular background trend in VLM.

To derive residual VLM and its uncertainties from GRACE observations and GIA estimates, multiple processing steps have to be taken, which are summarized in Figure 1. We use a Monte-Carlo approach through all processing steps to obtain uncertainties in all quantities. We first introduce the estimates of GIA and ~~PDMR in Paragraph~~ contemporary mass redistribution in paragraphs 2.1 and 2.2. Then, we briefly discuss the methodology to compute the resulting ~~regional~~ local RSL and deformation patterns in Paragraph 2.3. Finally, we discuss how these estimates are used to compute ~~VLM trends from GNSS observations in~~ linear trends in observed and residual VLM time series in Paragraph 2.4.

### 2.1 ~~The~~ GIA ~~model~~estimates

GIA ~~affects GRACE observations, causes solid-earth deformation,~~ causes changes in the gravitational potential observed by GRACE satellites, causes SED which affects VLM observed by GNSS stations, and causes ~~regional sea-level~~ local RSL changes, which are observed by tide gauges (**?**). To correct all these observations in a consistent way ~~,~~and to derive ~~uncertainties that result from the GIA correction~~robust uncertainties, we use the ~~GIA model ensemble from **?**. It does not only predict an estimate of the GIA-induced changes, but it also~~ ensemble of GIA estimates from C18, which provides a large ensemble of predictions, computed from varying the solid-earth parameters and the ice-sheet histories. Each ensemble member comes with

a likelihood that reflects its fitness to a global dataset of vertical ~~GPS~~ GNSS velocities and paleo sea-level records. Note that some circular reasoning is introduced here, as GNSS data was used to benchmark the GIA estimates. However, since the vast majority of the benchmark data comes from paleo indicators, and the cost function used to compute the likelihood is much more sensitive to paleo rather than GNSS data, the impact of this at first glance circular reasoning on the results is limited. From this ensemble, we ~~can derive~~ derive the mean and associated uncertainties for GIA-induced changes. We use a subset of 5,000 ensemble members from the original set that contains 128,000 GIA ~~models~~estimates. This number is sufficient to approach the original ensemble set with a maximum deviation of 2.5 percent from the original covariance matrix. Each ensemble member provides an estimate of the GIA ~~signal observed by GRACE and the RSL and deformation patterns. PDMR estimates, and also the GIA correction that must be applied to GRACE observations to obtain PDMR, are often expressed as a change in equivalent water height~~ effect on the gravitational potential, which we express in units Equivalent Water Height (EWH), an estimate of the solid-earth deformation, and an estimate of the RSL changes.

~~From this~~ To derive mean values and associated uncertainties from the ensemble, we ~~compute mean trends~~ use the likelihood $\mathcal{L}$ of each ensemble member. We can then compute the mean value $T_\mu$ and its uncertainty $T_\sigma$ ~~, weighted by the likelihood of each solution, as follows:~~ for the process of interest following:

$$T_\mu = \sum_{n=1}^{N} \frac{\mathcal{L}(n)}{\sum_{n=1}^{N} \mathcal{L}(n)} T(n)$$

$$T_\sigma = \sqrt{\sum_{n=1}^{N} \frac{\mathcal{L}(n)}{\sum_{n=1}^{N} \mathcal{L}(n)} \left(T(n) - T_\mu\right)^2},$$

where $N$ is the number of ensemble members, $T(n)$ the ~~trend~~ value of the individual ensemble member~~, and $\mathcal{L}$ the likelihood of each ensemble member~~. All uncertainties are on the $1\sigma$ level, unless otherwise specified. Note that the underlying probability density function (PDF) does not have to be Gaussian or symmetric. ~~To approximate the full~~ We can also derive an empirical PDF from the ensemble, from which confidence intervals at any level can be computed. To compute the empirical PDF, we ~~bin the quantity of interest (for example RSL), and then sum~~ first sort the values from low to high. Then we define 20 bins between the 1st and 99th percentile of these values and compute the sum of the likelihood of all ~~ensembles that fall into~~ ensemble members that fall within each bin. The ~~trends in EWH, deformation and RSL , together~~ number of 20 bins is chosen as a trade-off between resolution and sample size. The linear trends in the ensemble-mean EWH, SED and RSL with their uncertainty ~~estimate, are depicted~~ estimates are shown in Figure 2. The regions with the largest trends and uncertainties are around the former ice sheets, while the far-field trends and uncertainties are smaller.

### 2.2 GRACE estimates of ~~present-day~~ contemporary mass redistribution

To estimate ~~PDMR~~contemporary mass redistribution, we use the JPL GRACE Release 6 (RL06) mass concentration (mascon) solution (**?**). This solution provides monthly-mean estimates of EWH anomalies from March 2002 until June 2017, with some gaps at the beginning and end of the GRACE record and has a nominal spatial resolution of 3 degrees by 3 degrees. We only look into mass changes on land, and do not take ocean-bottom pressure changes driven by ocean dynamics into

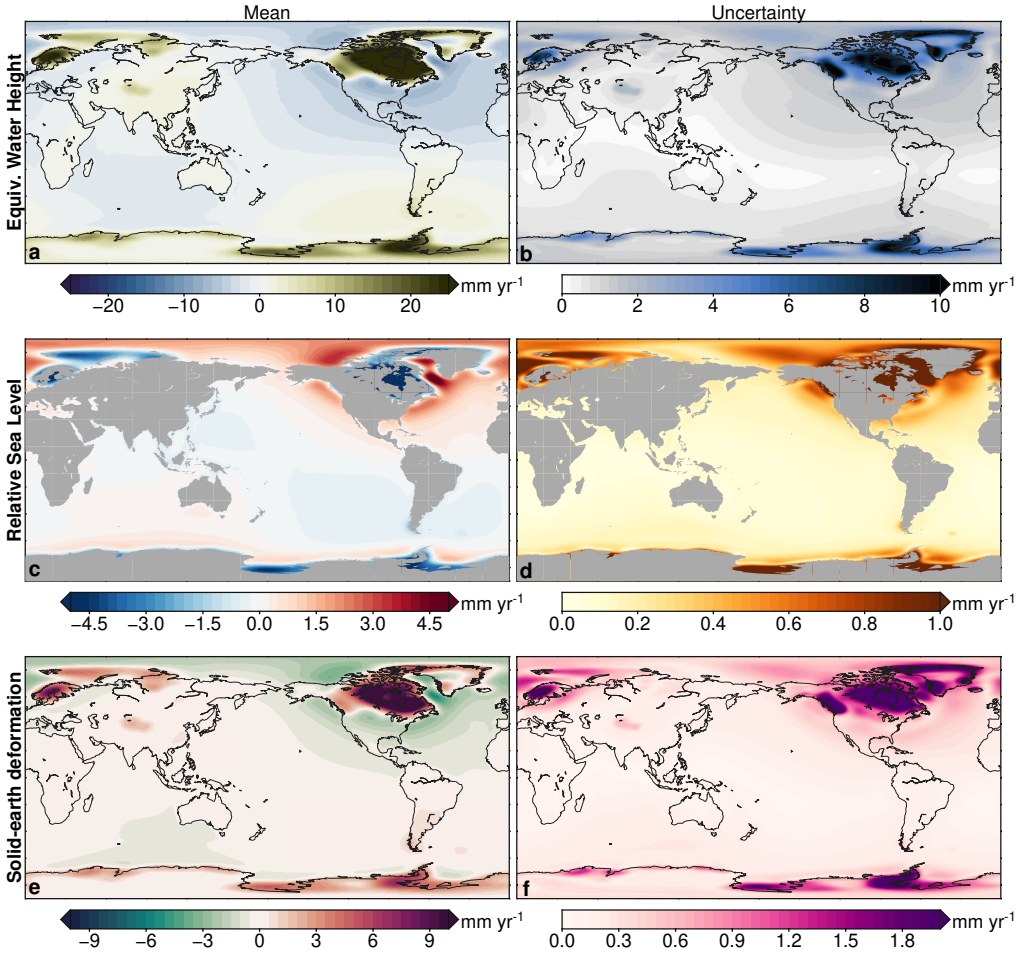


**Figure 2.** The ~~present-day~~ effects of GIA on contemporary linear trends ~~predicted by~~ in EWH (panels a,b), RSL (c,d), and SED (e,f) as estimated from the ~~large~~ 5000-member ensemble. The ~~top row shows EWH,~~ left panels show the ~~middle row shows RSL,~~ ensemble-mean and the ~~bottom row shows deformation~~right panel the $1\sigma$ uncertainty.

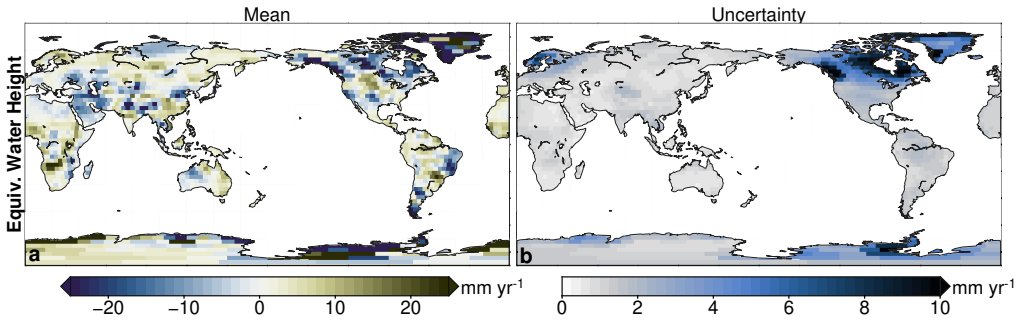


**Figure 3.** Trends and accompanying uncertainties in ~~the~~ contemporary EWH changes on land over 2002-2017, observed by GRACE. These trends have been corrected for GIA.

account, since its spatial variations are much smaller than the land mass changes (e.g. **?**). For mascons that contain a coastline, a Coastline Resolution Improvement (CRI) filter has been used to prevent the leakage of gravity signals between land and ocean, which leads to a better spatial representation of mass changes in coastal regions (**?**). The RL06 solution ~~is corrected for geoid perturbations caused by polar wander: movements in the earth axis of rotation (?), and~~ comes with an estimate of the measurement uncertainty of the EWH changes in each mascon.

We ~~apply the GIA correction from each ensemble member~~ first restore the original GIA correction applied to the GRACE ~~estimates, which yields~~ solution, and then we generate a 5000-member ensemble of GRACE EWH estimates~~. Each of these realizations is then~~ , each perturbed randomly using the ~~measurment~~ measurement uncertainty estimate in each mascon. These uncertainties are based on the formal error covariance matrix of the GRACE solutions, see **?** for details. This measurement uncertainty is given for each individual mascon and time step, and we assume that these uncertainties are uncorrelated in space and time. We then correct each perturbed mascon for GIA using one of the GIA ensemble members. Following **?**, we adjust the degree-2, order-1 terms of the GIA ~~model~~ estimates to account for the fact that GRACE observations are taken from an inertial reference frame, and not from the rotating ~~earth. From this ensemble, we~~ Earth.

With this procedure, we now have 5,000 estimates of contemporary mass redistribution, from which we derive the expected ~~PDMR~~ contemporary mass redistribution and the associated uncertainty, as well as the total land mass change. Note that the uncertainty estimates of these trends are only based on the spread in the ensemble, and not on the uncertainty that arises from fitting a linear trend to the data. Since geophysical time series often exhibit serial correlation, this assumption results in an underestimation of the uncertainty of the resulting trends (**?**). Figure 3 shows the trends and associated uncertainties in the GRACE estimates. The uncertainty in the trend is dominated by the GIA uncertainty, as the spatial pattern is almost identical to the pattern shown in Figure 2b, and the measurement ~~uncertainty only reaches~~ uncertainties only reach values of about 1 mm $yr^{-1}$ EWH. ~~Note that the uncertainty estimates of these trends are only based on the spread in the ensemble, and not on the uncertainty that arises from fitting a linear trend to the data. Since geophysical time series often exhibit serial correlation, this assumption could result in an underestimation of the uncertainty (?).~~

To isolate the role of cryospheric and hydrologic processes, we separate the observed EWH changes into changes from the Greenland Ice Sheet, the Antarctic Ice Sheet, glaciers~~and ice caps~~, and TWS. The EWH changes on both ice sheets can be isolated by only selecting the mascons that ~~overlap with the~~ cover ice sheets. ~~In other mascons where both glaciers and TWS are potential contributors to the mass changes, a priori information is required to disentangle the components. To do so~~Glaciers tend to be smaller in size than ice sheets and glaciers often do not form the dominant source of mass redistribution in the mascons that contain glaciated regions. Therefore we cannot directly apply the separation per mascon. Instead, we use ~~the same~~ a similar approach as **?**. First, we determine ~~the mascons that overlap with~~ those mascons that contain glaciated regions, based on the Randolph Glacier Inventory (**?**). For mascons that do not overlap with a glaciated region~~or ice sheet~~, all mass changes are attributed to TWS changes. For the mascons that do contain glaciers, we distinguish three cases:

1. Mass changes from the peripheral glaciers of Greenland and ~~Antarctica~~ Antarctic are part of the mass balance of both ice sheets. ~~For glaciers and ice caps~~

2. For glaciers in Alaska, Arctic Canada, Iceland, Svalbard, the Russian Arctic and the Southern Andes ~~,~~ we assume that the mass changes in the associated mascons are solely caused by glacier mass changes. ~~For the~~

3. For all other glaciated regions ~~, we use the pentadal~~ we use we use the annual glacier mass balance estimates based on geodetic and glaciological measurements from ~~the GMBAL dataset (**?**, version R1501). The~~ **?** as the glacier mass change estimate. We then subtract this glacier contribution from the total mass change in ~~these mascons is separated into a glacier contribution from the GMBAL data set and a TWS contribution~~the mascon to obtain the TWS estimate. The annual estimates from **?** come with an estimate of the uncertainty. To propagate this uncertainty into the glacier and TWS mass balances, we perturb the annual glacier mass balance estimates for each ensemble member. Note that, contrary to **?**, we use the ~~GMBAL~~ in-situ estimates for the glaciers and ice caps in the high mountain Asia region, instead of the estimates from **?**, since the latter only covers the period 2003-2009, which would require an extrapolation of 8 years. ~~Figure 4 shows~~

Figure 4 gives an overview of the mascon geometry ~~, as well as the mascons of the ice sheet and glacier regions~~and shows the mapping of each mascon into the individual processes.

### 2.3 Solid-earth deformation and relative sea-level changes resulting from mass redistribution

~~PDMR causes in the regional earth gravity field (geoid changes, $G(\theta,\phi,t)$), deformation ($R(\theta,\phi,t)$), in RSL ($\eta(\theta,\phi,t)$) and in geocentric sea level ($\zeta(\theta,\phi,t)$). $\theta$ and $\phi$ denote latitude and longitude, and $t$ time. RSL is defined as a change of the sea surface relative to the underlying sea bottom, while geocentric~~ The aforementioned procedure results in an ensemble of 5000 estimates of monthly land-mass changes. To compute the resulting SED and RSL changes, we solve the sea-level ~~change is a change of the sea surface, relative to the center of the earth. These changes have the following relationship:~~

$$\eta(\theta,\phi,t) = \mathcal{M}(t) + G(\theta,\phi,t) - R(\theta,\phi,t)$$
$$\zeta(\theta,\phi,t) = \mathcal{M}(t) + G(\theta,\phi,t) = \eta(\theta,\phi,t) + R(\theta,\phi,t).$$

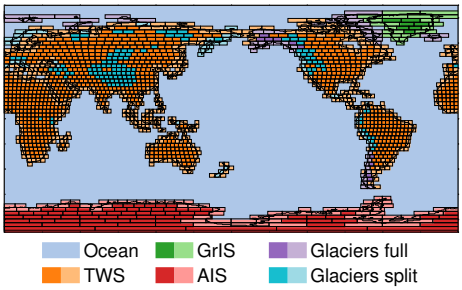


**Figure 4.** Overview of the GRACE mascon geometry and mascons associated to Greenland Ice Sheet (GrIS), Antarctic Ice Sheet (AIS), ~~glacier and ice cap (GIC)~~glaciers, and TWS mass changes. The light-colored mascons denote mascons which partially cover oceans and use the CRI filter. Mass changes in purple mascons (~~GIC~~ glaciers full) are fully attributed to glaciers, while turquoise mascons (glaciers split) are separated into a glacier and TWS term, see text.

~~The term $\mathcal{M}$ is needed to ensure that the total mass of the earth system is conserved. Note that this term is not necessarily equal to the barystatic sea-level change, which is the global-mean change in $\eta$ (not $\zeta$, since changes in $R$ could make the global-mean ocean deeper or shallower) due to mass entering or leaving the ocean, and equals 1 mm for each 362 Gigaton that enters the ocean. To compute these changes, we~~ equation (**?**) for each ensemble member. We use the pseudo-spectral approach (**?**), which requires the land mass changes to be transformed into spherical harmonics. We apply this transformation using the SHTns library (**?**) up to degree and order 180. We solve the sea-level equation ~~(?), using the pseudo-spectral approach (?)~~in the centre-of-mass reference frame and apply the rotational feedback (**?**). We assume that the solid-earth response to ~~PDMR~~ contemporary mass redistribution is purely elastic, and thus differs from ~~viscoelastic~~ visco-elastic GIA. We ~~solve the sea-level equation in the centre-of-mass reference frame, up to degree and order 180, and include the rotational feedback. We~~ use the elastic love numbers from **?**, which are based on the Preliminary Referenced Earth Model (PREM, **?**). ~~We solve the sea-level equation for each ensemble member, which results in~~ This procedure results in an ensemble of 5000 estimates of ~~deformation~~ local SED and RSL at each ~~grid cell and~~ GRACE time step. ~~GNSS receivers measure deformation $R(\theta,\phi,t)$ as VLM, while tide gauges measure relative sea level $\eta(\theta,\phi,t)$. Hence, tide-gauge observations that are corrected for the full VLM trend measure geocentric sea level $\zeta(\theta,\phi,t)$. This is also the case for tide-gauge records that are corrected for VLM using the difference between altimetry and tide-gauge observations (?).~~

### 2.4 GNSS stations and VLM trend estimates

We use the GNSS dataset from the University of Nevada, Reno (**?**, geodesy.unr.edu), which provides processed daily time series of over 14000 permanent GNSS receivers in the ITRF2008 reference frame. For consistency, we only use observations that overlap with the GRACE era (2002-2017). We remove stations for which less than 1825 daily observations that overlap with the GRACE era (2002-2017) are available, which corresponds to a minimum record-length of five years. This requirement, which is a trade-off between accuracy and data availability, results in a total of 8228 stations. Figure 5 shows a histogram of the

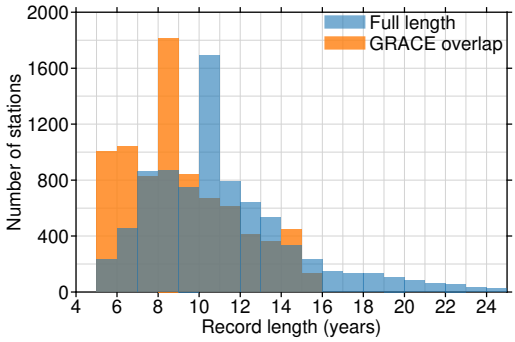


**Figure 5.** Histogram of the record length per station. Shown are all stations that fit the criteria outlined in paragraph 2.4. The blue bars show the record length before removing data outside the GRACE time span, and orange after removing.

record length per station, both before and after removing the observations that fall outside of the GRACE era. The histogram shows that most GNSS stations have a record length of around 8 to 10 years, or about half the length of the GRACE time span. Only a small fraction of the GNSS stations cover the full GRACE era. Since we only consider the observations within the GRACE era, not all data can be used, which results in a decrease in the record length that is available for some stations. We interpolate the monthly VLM that results from ~~deformation due to PDMR~~ SED due to contemporary mass redistribution and GIA on the GNSS time steps, which enables us to separate the full GNSS time series into its components ~~:~~

$$z_{\text{obs}}(t) = R_{\text{GIA}}(t) + R_{\text{cryosphere}}(t) + R_{\text{TWS}}(t) + z_{\text{residual}}(t),$$

~~with $z_{\text{obs}}(t)$ the observed height anomaly at time $t$, and $R_{\text{GIA}}(t)$, $R_{\text{cryosphere}}(t)$, and $R_{\text{TWS}}(t)$ the uplift caused by deformation due to GIA, ice sheets and glaciers, and TWS. $z_{\text{residual}}(t)$ is the residual anomaly, which is the observed height anomaly that cannot be explained by the other terms. Combining Equation 3with Equations 4 and 2 shows that removing the full GNSS observations $z_{\text{obs}}(t)$ from the tide-gauge observations, the resulting time series denotes geocentric sea level ζ~~and the residual VLM following Equation 3.

~~Deformation due to GIA and PDMR could cause a net uplift or subsidence of the global and regional ocean bottom, and the total volume change of the oceans differs from the ocean volume change directly inferred from geocentric sea-level changes. This difference results in a bias when global or regional sea-level changes are estimated from VLM-corrected tide-gauge records. Both GIA and contemporary mass redistribution result in a global-mean ocean bottom subsidence: for GIA, the global-mean subsidence is about 0.3 mm yr$^{-1}$ (?), and for contemporary mass redistribution the subsidence is in the order of 0.1 - 0.2 mm yr$^{-1}$ over the last 25 years (?). On regional scales, the difference between ocean-volume changes and geocentric sea-level changes can even be larger (?). Using the trend in $z_{\text{residual}}(t)$ to correct tide-gauge records for VLM avoids this bias, since ocean-bottom deformation resulting from GIA and PDMR has been removed from the VLM records. As a result, tide gauges corrected with $z_{\text{residual}}(t)$ denote relative sea level with respect to GIA and PDMR, while local VLM signals from other processes, such as tectonics and local subsidence are removed from the record.~~ To estimate linear trends in the observed and residual height anomalies, we apply the MIDAS robust trend estimator (?) to the observed and residual height anomalies. The

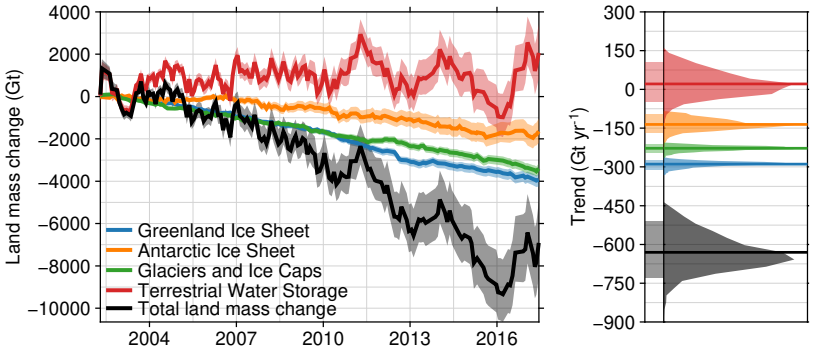


**Figure 6.** Total land mass changes as observed by GRACE, corrected for GIA. The left panel shows the expectation (thick line) and 90% confidence intervals (shade) of the mass change time series for each process and the total land mass change. Negative values denote land mass loss. The right panel shows the expected value (thick line), 90% confidence interval (left shade) and PDF (right shade) of the resulting linear trend.

MIDAS estimator does not compute the linear trend using linear least squares, but based on the median of the height difference of each pair of anomalies that are separated by 1 year, while the uncertainty estimate is based on the standard deviation of the 1-year separated anomaly differences. This approach has two advantages over the classical approach: ~~1. it~~ It is less sensitive to discontinuities in the time series, which are omnipresent in GNSS records (**?**), and ~~2. is is~~ it is computationally less expensive than least-squares estimation using an appropriate serially-correlated noise model. ~~We estimate the trends for the full ensemble to obtain an uncertainty estimate for each trend~~To propagate the SED uncertainty into the residual VLM trends, we estimate the MIDAS trends for each ensemble member and GNSS station, which results in two sources of uncertainty: the spread in the residual VLM trends due to SED and the uncertainty that results from estimating linear trends from noisy GNSS data. We assume that the uncertainty from the trend estimator and the ensemble spread are independent, and these terms are added up in quadrature to obtain the final uncertainty.

## 3 Results

### 3.1 Global-mean land-mass changes

The global-mean land-mass changes due to ~~PDMR~~ contemporary mass redistribution are shown in Figure 6 ~~, which shows that , while~~ and Table 1, which show that all cryospheric processes ~~causes~~ cause a net land mass loss, ~~the TWS term causes land mass gain. The~~ while TWS does not show a significant positive or negative linear trend. Over the first decade of the GRACE era, a positive TWS term has been observed ~~over the first decade of GRACE observations~~ by **?** and **?**, ~~and the trend continues to be positive over the full GRACE record~~ although the land mass loss over the last few years of the GRACE record has resulted in a trend that does not deviate significantly from zero. For all cryospheric processes, the total mass changes are dominated by the trend, and the variability around the longer-term trend is relatively small ~~, while for TWS, the~~ compared to TWS, whose

**Table 1.** Trends in land mass changes and corresponding barystatic sea-level changes. The numbers in brackets show the uncertainties expressed as the corresponding 5-95% confidence intervals. A positive sign for the mass change correspond to increase of the mass on land, and a positive sign of the barystatic trend denotes a global-mean sea-level rise.

| | Mass change (Gt $yr^{-1}$) | | Barystatic sea-level change (mm $yr^{-1}$) | |
|---|---|---|---|---|
| Greenland Ice Sheet | ~~−290~~ −289 | ~~[−312 ; −272]~~[−309 ; −273] | 0.80 | ~~[0.75 ; 0.86]~~[0.75 ; 0.85] |
| Antarctic Ice Sheet | ~~−144~~ −135 | ~~[−176 ; −108]~~[−168 ; −97] | ~~0.40~~ 0.37 | ~~[0.30 ; 0.49]~~[0.27 ; 0.47] |
| Glaciers ~~and Ice Caps~~ | ~~−238~~ −228 | ~~[−250 ; −227]~~[−245 ; −212] | ~~0.66~~ 0.63 | ~~[0.63 ; 0.69]~~[0.59 ; 0.68] |
| Terrestrial Water Storage | ~~100~~ 21 | ~~[42 ; 171]~~ [−47 ; 105] | ~~−0.28~~ −0.06 | ~~[−0.47 ; −0.11]~~[−0.29 ; 0.13] |
| Total land mass change | ~~−572~~ −630 | ~~[−659 ; −465]~~[−729 ; −508] | ~~1.58~~ 1.74 | ~~[1.28 ; 1.82]~~[1.40 ; 2.01] |

inter-annual variability around the mean trend is substantial, especially after 2010. It is known that TWS exhibits substantial decadal and multi-decadal variability (**??**), and a large part of this variability corresponds to the strong ENSO cycles during this period, which are known to have a large effect on water stored on land (**??**).

The uncertainties in the trend and time series for Greenland and glaciers are smaller than the uncertainties for Antarctica and TWS. This difference is caused by the uncertainty in the GIA contribution, which is small for Greenland and most glaciated regions, ~~and~~ while the GIA contribution is larger and more uncertain for the Antarctic Ice Sheet. The uncertainty in the TWS term is largely caused by the uncertainty in the GIA contribution from the former Laurentide Ice Sheet, which covered large parts of North America (see Figure 3). Due to this uncertainty, the partitioning of the observed EWH changes over North America between GIA and ~~present-day~~ contemporary changes is uncertain, which leads to a large spread in the possible TWS contribution from this region. The distributions shown in Figure 6 are not symmetric, which causes slightly skewed confidence intervals in Table 1. The total land mass ~~mass~~ loss over the second half of the record is larger than the loss over the first half, which is caused by the accelerating contributions from Greenland and Antarctica, and the slowdown of the TWS contribution. ~~The linear trends in total land mass change and the individual components are shown in Table 1, which also contains the resulting barystatic sea-level trends. The total land mass trend over the GRACE era is negative. TWS is the smallest term, but has the largest uncertainty. The distributions shown in Figure 6 are not symmetric, which causes slightly skewed confidence intervals in Table 1. The trends in the individual terms are consistent with recent studies (**???**)~~The trends in the individual terms are consistent with recent studies (**??**), although quantifying TWS changes without GRACE is still challenging (**?**), which still hinders the validation of GRACE-based TWS changes.

### 3.2 ~~Regional~~ Local patterns in relative sea level and solid-earth deformation

As discussed in Section 2.3, the mass changes will lead to ~~regional RSL and deformation~~ local RSL and SED patterns. Figure 7 shows the ~~trends in regional RSL resulting from TWS and cryopsheric processes, together~~ resulting trends in local RSL with the accompanying uncertainty. As expected from the barystatic contribution (Figure 6), the ~~trends in sea level~~ RSL trends are dominated by cryospheric processes, while the TWS-induced ~~trend in sea level~~ RSL trend is generally no more than a few tenths of millimetres per year and has a less-pronounced ~~regional pattern. However, the TWS contribution shows substantial~~

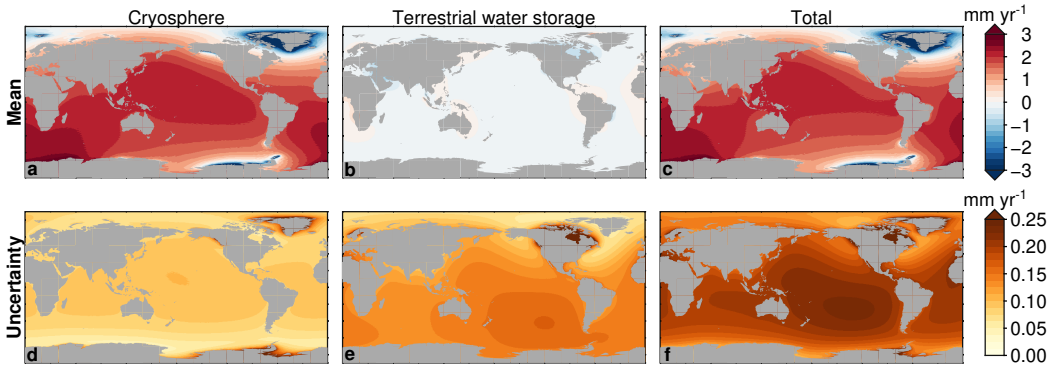


**Figure 7.** Trends in ~~relative sea level~~ RSL resulting from mass redistribution observed by GRACE, separated into the cryosphere contribution (sum of glacier and ice sheet contribution), the TWS contribution, and the total land mass contribution. The trends have been computed over the full GRACE time span (2002-2017). The top row shows the mean trend, and the bottom row shows the uncertainty.

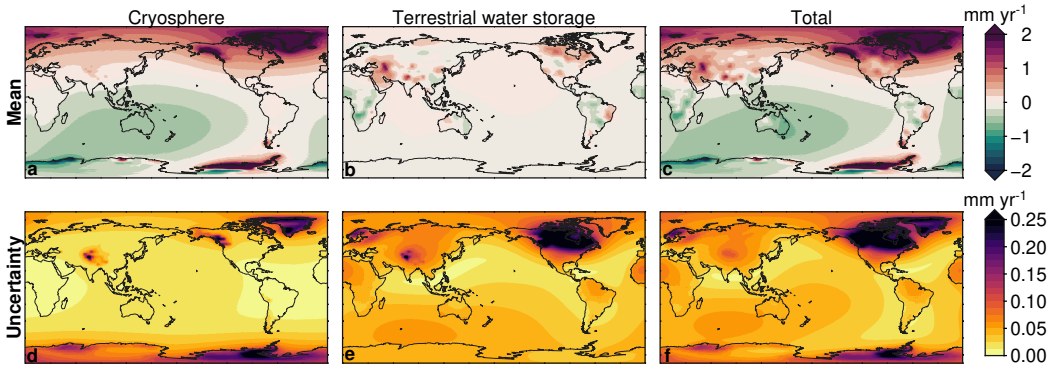


**Figure 8.** Trends in ~~deformation~~ SED resulting from mass redistribution observed by GRACE, separated into the cryosphere contribution (sum of glacier and ice sheet contribution), the TWS contribution, and the total land mass contribution. The trends have been computed over the full GRACE time span (2002-2017). The top row shows the mean trend, and the bottom row shows the uncertainty.

~~variability around the long-term trend, both for the barystatic contribution, as well as for local changes. The uncertainty in these fingerprints is~~ spatial pattern. The local uncertainties are dominated by the TWS contribution~~, and for~~ . For large parts of the ocean, the uncertainty in the TWS contribution has a similar magnitude as the trend. The uncertainty ~~for the~~ in cryosphere-induced local ~~sea-level~~ RSL changes is limited to about 0.1 mm $yr^{-1}$, except for regions very close to glaciers and the ice sheets. The uncertainty of the total signal is again on the order of 0.1 - 0.2 mm $yr^{-1}$, which is substantially smaller than the signal itself.

~~The regional deformation trends are depicted in Figure 8 . Next~~ Figure 8 shows that, next to uplift at locations where the ice-mass loss takes place, mass changes in the cryosphere result in ~~considerable~~ some far-field ~~deformation signals, and causes~~ SED signals, including subsidence of about 0.5 mm $yr^{-1}$ ~~in~~ around Australia, and ~~uplift in large parts of Europe~~

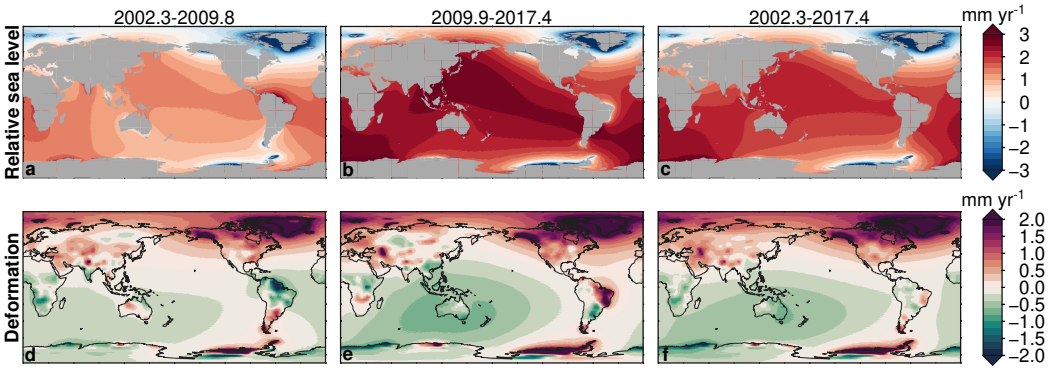


**Figure 9.** Trends in RSL (~~top row~~a-c) and ~~deformation~~ SED (~~bottom row~~d-f) resulting from the total mass redistribution observed by GRACE over the first (~~left~~a,d) and second half (~~center~~b,e) of the GRACE observation, and the total GRACE period (~~right~~c,f). Note that ~~deformation~~ SED related to GIA is not included here.

~~and North America~~an uplift signal with a similar magnitude in Europe and Northern Asia. TWS changes cause considerable near-field ~~deformation~~ SED trends, for example in South America and Asia. Both uplift and subsidence occur, which shows that the barystatic trend consists of the sum of regions of land mass loss and land mass gain, and as such, the TWS-induced ~~deformation~~ SED signals, which have a predominantly near-field signature, will likely not follow the ~~global-mean variability . The deformation~~ variability in the barystatic contribution from TWS. The SED uncertainty is large close to former glaciated regions due to the local impact of GIA. For other regions, the uncertainty is below the 0.1 mm $yr^{-1}$ level, also for the locations for which the local trend is large.

The TWS-induced total land mass change shows substantial temporal variability, and the mass loss at both the Greenland and Antarctic ice sheets is accelerating. Therefore, linear RSL and ~~deformation~~ SED trends, derived over a subset of the GRACE period are likely to deviate from the trends derived over the full period. As an example of the size of these deviations, Figure 9 shows the ~~RSL and deformation~~ linear RSL and SED trends over the first and second half of the GRACE era, both covering 7.5 years. As a result of ~~this increasing~~ the accelerating barystatic sea level trends, the ~~regional~~ local RSL trends are overall larger ~~in amplitude~~ during the second half of the GRACE era, although the spatial pattern only shows limited changes between the different periods. In contrast, local ~~deformation~~ SED trends, mostly associated with TWS changes, show vast differences between both periods. Notable regions include the Amazon basin and southern Africa, who subside over the first half of the period and show uplift over the second half of the GRACE period. The opposite occurs in the Rio de la Plata basin and Northwest Australia. ~~In these regions, the deformation measured by the GNSS receivers depends substantially~~ Linear trends in SED thus do depend on the time span ~~of the record and as a result, nearby stations could see different trend when they cover different periods~~over which these trends are computed, which implies that due to SED, extrapolating a linear trend in VLM will cause biases.

### 3.3 The role of solid-earth deformation in observed VLM trends

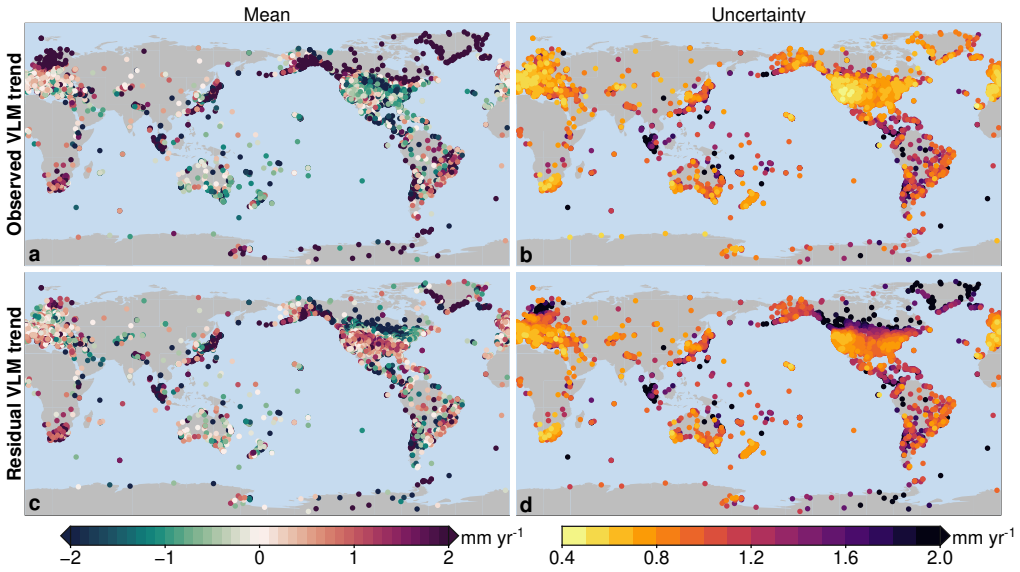


**Figure 10.** Observed VLM and residual VLM trends from GNSS records. Panels a,b: the trend in observed VLM and associated uncertainty. c,d: Trends in residual VLM after removing the SED effects due to GIA and contemporary mass redistribution. All trends have been computed over the time spans for which GNSS and GRACE observations overlap.

~~As discussed in the previous section, the deformation trend depends substantially on the time span of the GNSS observation.~~ The linear trends in GNSS records (Figure 10a) do show substantial spatial variability, even for nearby stations, although the uncertainty, which generally exceeds 0.5 mm/yr due to the short GNSS records, noisy data, and the presence of jumps in the data (**?**), should be considered when comparing nearby stations. Nevertheless, the observed VLM trends show many well-known large-scale features, mostly associated with GIA and uplift associated with contemporary ice mass loss. To quantify the role of ~~deformation~~SED in actual VLM trends as observed by GNSS stations, we computed the ~~trend~~ linear SED trends over the time span of each GNSS station (Figure 11).

The cryosphere-driven ~~deformation~~ SED trends mostly show smooth ~~temporal and~~ spatial variations, ~~which suggests~~ and compared to the trend, the inter-annual variations are small, which implies that the specific time span of the GNSS record has a limited impact on the observed ~~deformation rate~~linear trend in SED. Cryosphere-induced ~~deformation results in substantial trends~~ SED results in linear trends of a few tenths of a millimetre per year or larger at many GNSS stations~~: not only~~ . These trends do not only reflect the well-known near-field uplift signals at or near the ice-mass loss locations, which dominate the VLM signal for many regions where ice mass loss occurs, but also in the far field, with notable uplift in large parts of Europe and the US, and subsidence in Australia. The uncertainty of these trends is negligibly small, except for the stations close to the locations of ice mass loss.

In contrast, the TWS-induced ~~deformation~~ SED trends show a less smooth pattern: sharp contrasts in the trends between nearby stations can for example be seen in North and South America, owing to the aforementioned difference in the time span

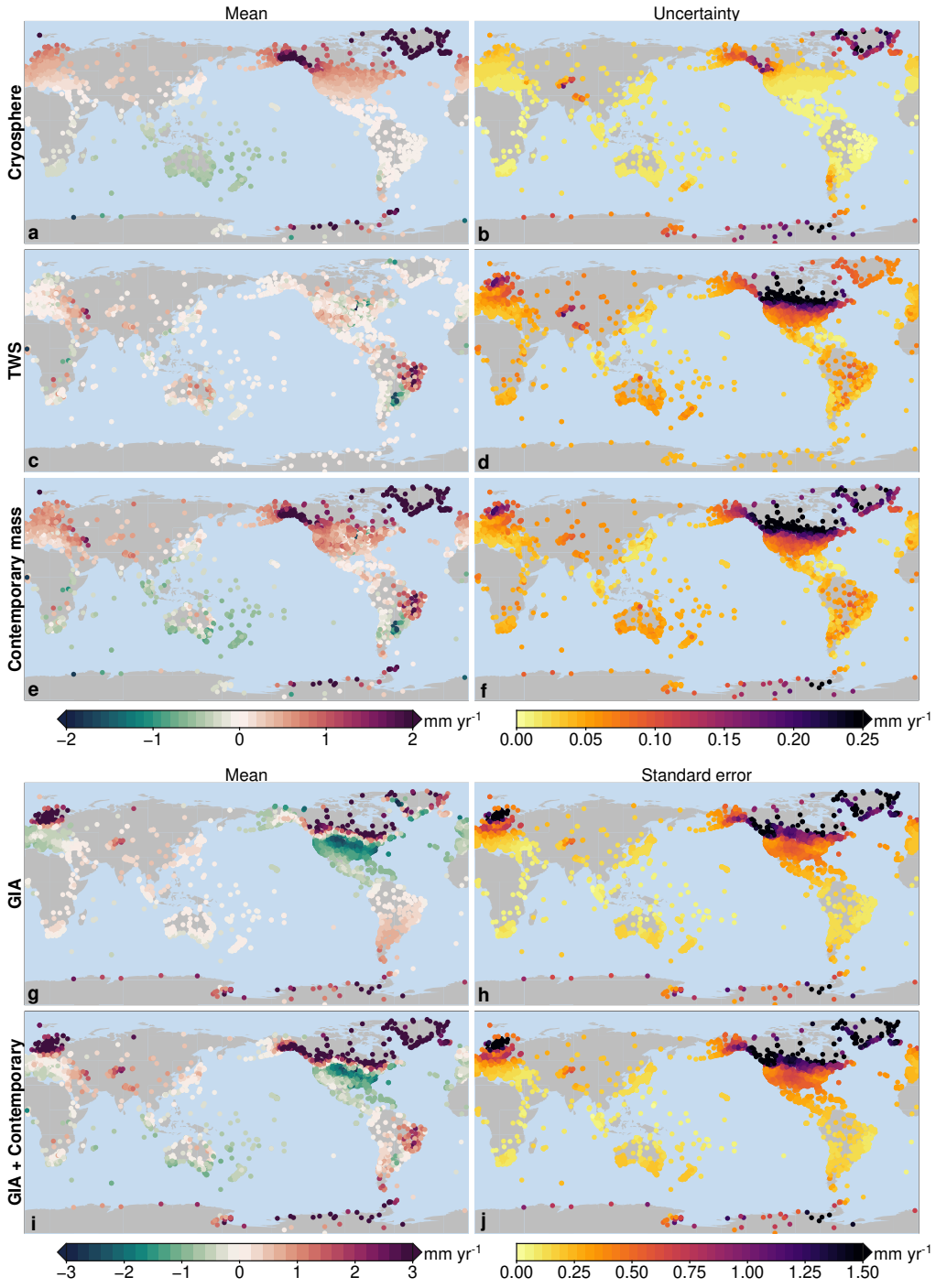


**Figure 11.** The modelled linear trends due to ~~deformation~~ SED computed over the time span of the individual GNSS record. The left panels show the mean trend, and the right panels the uncertainty from the large ensemble. Note that the color scales for the top three rows ~~differs~~ differ from the color ~~scale~~ scales of the bottom two rows.

of the GNSS records and the TWS trends that depend on the period over which these trends are computed. ~~GNSS stations along the coastlines generally witness smaller deformation trends related to TWS changes, because these stations are located along the edges of the TWS load change regions, instead of in the middle. Nevertheless, deformation trends~~ SED trends at coastal locations can be substantial, which points at possible biases when VLM estimates used to correct tide-gauge observations do not account for TWS-induced ~~deformation~~SED. For many regions, the ~~deformation~~ SED trend is dominated by GIA, especially for the ~~Northeastern~~ North-eastern parts of North America and Northern Europe, while for South America and Australia, ~~PDMR~~ contemporary mass redistribution is the dominant ~~deformation~~ SED component. Not only the ~~deformation~~ SED trends, but also the associated uncertainties are mostly driven by the GIA. Outside regions with a notable GIA signal, the uncertainties in the trends are small.

~~When we apply Equation 3 to the GNSS observations, we can remove deformation due to PDMR and GIA from the GNSS observations. The original and residual GNSS trends are shown in Figure 10. Observed VLM trends from permanent GNSS stations, together with the uncertainty. Top row: the original time series. Bottom row: time series corrected for modelled deformation due to GIA and PDMR. Both trends have been computed over the time spans for which GNSS and GRACE observations overlap. The trends in GNSS records do show substantial spatial variability, even for nearby stations, although the uncertainty, which is generally substantial due to the short GNSS records, noisy data, and the presence of jumps in the data (?), should be taken into account when comparing nearby stations. Nevertheless, the uncorrected GNSS trends show many well-known large-scale features, mostly associated with GIA and uplift associated with present-day ice mass loss. The~~ The removal of all modelled ~~deformation signals (Bottom panel in Figure 10~~SED signals (Figure 10c) highlights regional differences: for Europe, Australia and South America, ~~deformation~~ SED explains a large part of the observed large-scale VLM features, while for North America, a different pattern emerges, with an uplift signal over large parts of the United States. This uplift could have its cause in the GIA ~~correction~~estimates: the ensemble mean predicts a substantial subsidence pattern over large parts of North America, associated with the collapse of the Laurentide forebulge (Figure 2e), which is stronger than projected from some other models, such as ICE6G-VM5a (**?**)~~, even considering the uncertainty~~. For most cryospheric regions, the trends change, but a substantial residual signal remains. A possible explanation for this large residual is the fact that both the GIA ~~model~~ estimates and the GRACE ~~mascon solution provide PDMR~~ observations provide contemporary mass redistribution estimates at relatively coarse spatial resolutions, while it is known ~~in these regions that deformation~~ that SED induced by GIA and ~~present-day~~ contemporary ice mass loss can have a very local character in these regions due to localized mass changes and complex ~~earth structures (e.g. **??**)~~Earth structures (e.g. **??**). Some large-scale VLM features visible in the GNSS trends cannot be explained by the modelled ~~deformation~~SED. For some regions, such as Japan and Chile, tectonic activity is a likely candidate, but the uplift in Southern Africa is unlikely to be tectonic in nature. Nevertheless, ~~in general, the model explains a substantial part of the observed vertical land motion: the~~ the scatter plot in Figure 12 shows that the ~~modelled~~ SED trend for most stations is close to the observed VLM trend, although there are multiple stations that show large trends that are not explained by the model. Given the fact that many relevant local processes, such as tectonics and local subsidence are ~~not modelled~~still present in the residual VLM trend, these outliers are not surprising. The mean linear trend for all 8166 stations is 0.34 mm $yr^{-1}$ with a standard deviation of 4.46 mm $yr^{-1}$, while the mean residual trend is 0.44 mm $yr^{-1}$ with a

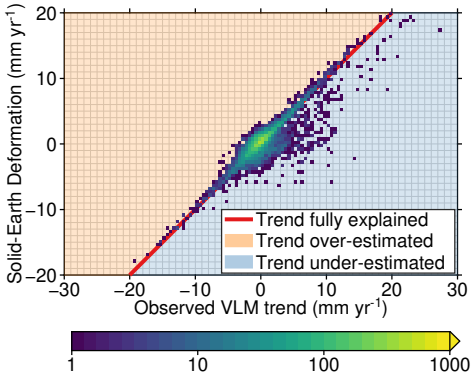


**Figure 12.** Scatter plot of observed ~~versus modelled~~ VLM trends (Figure 10a) versus the trend in ~~vertical land motion~~SED resulting from GIA and contemporary mass redistribution (Figure 11i). The color denotes the number of stations for each trend pair within 0.5 mm yr$^{-1}$. For points on the red line, the ~~modelled and~~ observed VLM trend and SED trend agree completely, in the orange area, the ~~modelled~~ SED trend is larger than the observed VLM trend, and for the blue area, the ~~modelled~~ SED trend is smaller than the observed VLM trend.

standard deviation of 4.28 mm yr$^{-1}$. The coefficient of determination ($R^2$) of the modelled trends is just 7.5 percent. The full list of stations also contains many stations for which the MIDAS estimates very large uncertainties, sometimes exceeding 10 mm yr$^{-1}$. If we limit our station selection to those stations for which the uncertainty in the observed VLM trend is smaller than 1 mm yr$^{-1}$, which is the case for 4252 out of 8166 stations, we obtain a coefficient of determination of 34 percent and a reduction of the standard deviation from 2.30 to 1.86 mm yr$^{-1}$.

### 3.4 Solid-earth deformation and long tide-gauge records

To ~~determine the effects of vertical land motion on trends from long-term~~ demonstrate the impact of SED on tide-gauge ~~records, we partially repeat~~ observations, we revisit the analysis of **?**, T16~~, which determines trends from~~. In this study, linear trends from from a set of 15 long-term tide-gauge records ~~. Since some of the stations from~~ are compared to multiple recent global-mean sea-level reconstructions. A discrepancy was found between the long tide-gauge records and most reconstructions, including the recent reconstructions from **?** and **?**. This study did not use GNSS observations to correct tide-gauges for local VLM. Here, we determine whether observed and residual VLM explain a part of this discrepancy.

For many of these stations, long VLM records from nearby GNSS stations are available. Some stations from that study are not in the ~~vicinity of a~~ vicinity (i.e. more than 50 km) of any GNSS station with a long record ~~(Cristobal),~~ or the combination of VLM and the tide-gauge trend results in an unrealistically low sea-level trend~~(Newlyn, Fremantle), we~~. We have removed these stations ~~,~~ and added nearby stations as a replacement ~~,~~ where possible. ~~See the supporting information for a complete overview of changed stations~~ Supporting Information Text S1 gives an overview of the stations that differ from T16 with an explanation of the reason, and Table S1 lists all tide-gauge stations together with the GNSS stations used to determine the local VLM trends. The linear trends in local sea level have been computed from annual tide-gauge data obtained from the Permanent Service for Mean Sea Level (**??**) using the Hector software (**?**), while assuming a power-law spectrum for the

temporally-correlated noise in each tide-gauge record. To stay consistent with T16, we only use annual tide-gauge data from 1901-2000.

We ~~apply three different corrections to the~~ compute linear trends in the uncorrected tide-gauge ~~trends~~record, and we compute the trend by applying three different correction models. In the 'GIA removed' model, the ensemble-mean GIA RSL trend ~~from the ? model~~ is removed from the tide-gauge trend. For the 'VLM removed' model, the ~~uncorrected GNSS~~ observed VLM trend is removed from the tide-gauge trend. ~~For the~~ 'Both the 'GIA removed' and the 'VLM removed' models are commonly used as a correction to tide-gauge observations (e.g. **?**). In the 'full' model, we remove both the ~~deformation-corrected GNSS~~ residual VLM trend, as well as the ~~modelled~~ GIA RSL trend. The ~~sea-level trends have been computed from annual sea-level data obtained from the Permanent Service for Mean Sea Level (??) using the Hector software (?), assuming a power-law spectrum~~'full' model removes the spatial variations due to GIA and local VLM not related to SED, while it avoids the extrapolation of the non-linear SED signal due to contemporary mass redistribution. In the 'full' model, sea-floor deformation signals due to contemporary mass redistribution and GIA are also retained in tide-gauge records. The uncertainties ~~due to~~ in the VLM and GIA ~~corrections~~ estimates are derived from the ~~large~~ ensemble, and subsequently added in quadrature to the uncertainty in the linear trend from the tide-gauge ~~uncertainties. To stay consistent with T16, we only use annual tide-gauge data from 1901-2000.~~ record. Figure 13 shows the ~~uncorrected and corrected trends for the stations, as well as their location. Linear trends in long tide-gauge records (1901-2000), with various corrections applied for vertical land motion. Blue: no correction, green: GIA RSL removed, yellow: original GNSS trend removed, red: GIA and corrected GNSS trend removed. The dashed lines show the median trend for each correction. The right pane shows the locations of the tide gauges. The black bars denote the 1 $\sigma$ uncertainties From the individual trends, we computed the mean and the standard deviation, which are shown in Table ??. As a~~ resulting linear trends at each station. For comparison, we also computed the trends for the 'GIA removed' and ~~'Full'~~ full' models using the ICE6G-D VM5a model ~~(??)~~(?), which is an updated version of the ICE6G-C VM5a GIA model (?) used in T16. ~~The 'GIA removed' and 'VLM removed' trendsboth have a lower standard deviation than the~~

From the individual trends, we computed the mean and the inter-station spread, which we express as the standard deviation between the trends from each tide-gauge station (Figure 13). All correction models reduce the spread between the stations, compared to the uncorrected trends. ~~This reduction due to the GIA correction was also found by T16.~~ Removing the ~~uncorrected~~ observed VLM trends from the tide-gauge trends also reduces the inter-station ~~standard deviation~~spread in the trends, although to a lesser extent than the 'GIA removed' model. ~~However,~~ All three correction models do reduce the station-mean trend from the 1.7 mm yr$^{-1}$ in the 'uncorrected' model. The 'VLM removed' model has the lowest mean trend (1.1 mm yr$^{-1}$), but this correction suffers from the two aforementioned problems: the linear trend due to ~~deformation~~ SED over the GNSS record is not representative for the full tide gauge record and the ~~ocean-bottom~~ sea-floor deformation signal is removed from the tide-gauge data. ~~These issues are both resolved using the 'full model', and it even further reduces the spread between stations. Mean and standard deviation of the trends from the long tide-gauge records shown in Figure 13 for each VLM correction. The standard deviation is calculated between the individual stations. The mean and standard deviation using the ICE6G-D VM5a model to correct for GIA are also listed for comparison. Mean (mm yr$^{-1}$) St. dev. (mm yr$^{-1}$) Original 1.66 0.59GIA removed 1.39 0.45 VLM removed 1.07 0.56 Full model 1.31 0.36 GIA removed (ICE6G) 1.54 0.35 Full model (ICE6G) 1.36 0.39~~

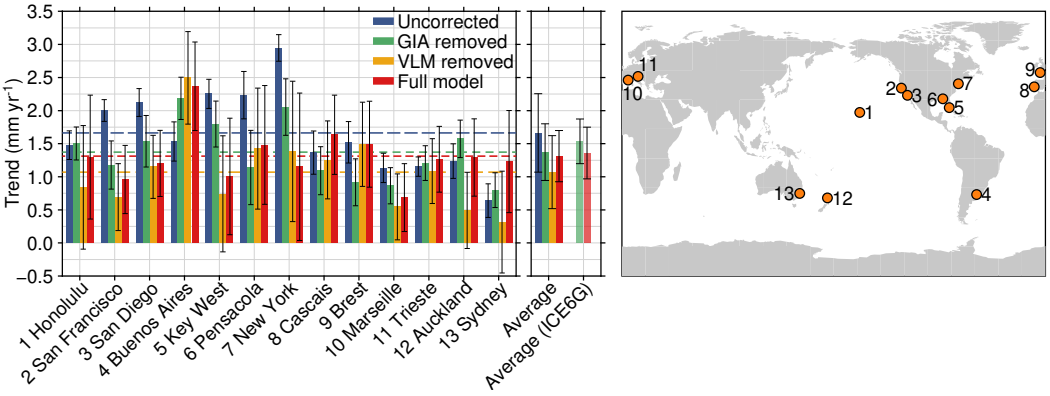


**Figure 13.** Linear trends in long tide-gauge records (1901-2000), with various correction models applied for vertical land motion. Blue: no correction, green: GIA RSL removed, yellow: observed VLM trend removed, red: GIA and residual VLM trend removed. The middle pane and the dashed lines show the median trend for each correction. The error bars in the middle pane denote the inter-station standard deviations of the trends for each model. The right pane shows the locations of the tide gauges. The black bars denote the 1 $\sigma$ uncertainties

~~Interestingly, the correction from the GIA ensemble reduces the mean sea-level trend at the tide-gauge locations by $\sim 0.3$~~ The latter effect explains the low mean trend for this method, as over the last few decades, due to contemporary mass redistribution, the sea floor has subsided by about 0.1 mm yr$^{-1}$ ~~, which is more than the $\sim 0.1$ mm yr$^{-1}$ from the correction based on the ICE6G-D model and the value found by T16. The removal of the uncorrected VLM trends results in a lower trend than the GIA-only correction. The~~ (**?**), which would result in an underestimation of GMSL if sea-floor deformation is not taken into account. The full model results in a ~~trend in beween the GIA-corrected and GNSS-corrected~~ station-average trend of 1.3 mm yr$^{-1}$, which lies in between the 'GIA removed' and 'VLM removed' models, but overall with the lowest ~~standard deviation of the four models~~inter-station spread. The mean trend of the full model is close to the trend found by **?** and **?**, who find a mean trend of ~~1.26~~ 1.3 mm yr$^{-1}$ and ~~1.21~~ 1.2 mm yr$^{-1}$ respectively over the 20th century. ~~Note that we do not take into account the spatial sampling bias that causes the~~ When we correct the tide-gauge records ~~discussed here to under-estimate the underlying 20th-century GMSL trend , as discussed in T16, so the gap discussed~~ for GIA using the ICE6G-D model, we find a station-mean trend of 1.5 mm yr$^{-1}$, which is close to the trend found by T16~~cannot be considered fully closed from these results. Also note that the 'full model' using~~ . The difference between C18 and ICE6G-D ~~for the GIA correction, instead of the **?** model, also results in a closer agreement between the long records and~~ points at the impact of the uncertainty in GIA models on tide-gauge trends. When we compare the full correction models, the difference between C18 and ICE6G-D again becomes much smaller, which shows that the residual VLM trend partially offsets the uncertainty in GIA estimates. Note that T16 also argues that averaging the linear trend in sea level from these long tide gauges likely underestimates the global-mean sea-level ~~reconstructions.~~ trend due to the spatial patterns associated with ice-mass loss and ocean dynamics. Here, we do not consider this spatial sampling bias, so the gap between the long tide-gauge records and global-mean sea-level reconstructions discussed by T16 cannot yet be fully reconciled from these results.

## 4 Conclusions

~~We have quantified the effects of PDMR on relative~~ We have developed an alternative approach to correct tide gauges for local VLM that reduces the aliasing of decadal and multi-decadal variability in contemporary mass redistribution into VLM trends estimates from short GNSS records. This method also avoids the bias when global-mean sea-level ~~change and VLM observations. The large ensemble of GIA predictions allows us to quantify the uncertainty that arises from this correction , and combined with the measurement uncertainties, we have derived estimates of RSL and deformation fingerprints, together with uncertainty estimates based on mass redistribution observed from GRACE. This approach also produces estimates of the total land-mass change, which, due to mass conservation, result in the opposite total mass change in the ocean . We find a total mass trend over the GRACE period between -659 and -465 Gt yr$^{-1}$, which corresponds to a mass-driven~~ changes are estimated from geocentric sea-level ~~trend between 1.28 and 1.82 mm yr$^{-1}$ (90% C.I.). This number is in disagreement with some other estimates of the total land mass change: **?** find a mean estimate of 2.3 mm yr$^{-1}$ from various methods to estimate GRACE mass changes. In our ensemble, no single realization can be reconciled with a mass change of 2.3 mm yr$^{-1}$. When evaluated over 2002-2014, we obtain a mean land mass trend of 1.4 mm yr$^{-1}$, which is consistent with the inversion approach of **?**, who find a mass trend of $1.1 \pm 0.3$ mm yr$^{-1}$ over 2002-2014. Our total mass trend is also consistent with estimates of the individual contributors, although the error bars remain substantial. This large spread between individual estimates has consequences for the sea-level budget, and a study to reconcile these differences would be a worthwhile exercise~~observations.

The ~~ensemble also allows for determining uncertainties for the resulting regional patterns of RSL and deformation trends. For the cryospheric processes, the trends in the regional patterns are an order of magnitude larger than the uncertainties, except for the formerly glaciated regions, where the uncertainty in the local GIA prediction plays a large role. For TWS , the uncertainties in relative sea level are generally of a similar magnitude as the trend. However, TWS~~ local solid-earth deformation signal due to contemporary mass redistribution depends on the location and the time span. Mass changes from ice sheets and glaciers cause large-scale deformation patterns, with far-field deformation patterns reaching values on the order of 0.5 mm yr$^{-1}$. TWS changes cause substantial ~~regional deformation~~ local SED trends, especially when computed over a subset of the whole GRACE time span. The ~~deformation~~ SED trends computed over the GNSS record time spans can reach values of more than 1 mm yr$^{-1}$, not only near melting ice sheets, but also in regions where large TWS changes occur, such as the Amazon Basin.

~~However, this approach comes with some limitations. The GRACE solutions have a limited temporal and spatial resolution. Since the mission only covers the period 2002-2017, GNSS observations from outside the GRACE period has been discarded, which, for some stations, substantially shortens the records, as displayed in Figure 5. This limitation means that the results of this study could be improved if deformation estimates are expanded to cover the full GNSS record. While for ice mass changes model results show good agreements with observations, estimating TWS changes, an important deformation source, remains challenging, which in turn limits the ability to use models to estimate deformation. Due to the coarse spatial resolution, sharp gradients in mass redistribution are smeared out over larger areas. Since deformation is sensitive to these local mass changes, the corrections computed here may under-estimate the local deformation in regions with strong spatial gradients. This issue~~

~~could be one of the reasons of the un-explained residual land motion around Greenland, Antarctica, and Alaska visible in Figure 10. Nevertheless, deformation resulting from GIA and PDMR explains a substantial part of the observed GNSS trends in~~ This solid-earth deformation resulting from GIA and contemporary mass redistribution explains a substantial part of the observed GNSS trends: for all 8166 stations, we obtain a coefficient of determination of 7.5 percent. When we only consider stations for which the standard error in the observed VLM trend is smaller than 1 mm $yr^{-1}$, the coefficient of determination becomes 34 percent. This difference suggests that a non-negligible part of the residual VLM trends can be attributed to the uncertainty in the estimated linear trends in VLM from noisy GNSS data, and that the uncertainties should not be overlooked when applying the observed and residual VLM trends to tide-gauge data. In multiple regions, including South America, Australia, and Europe, large-scale patterns of observed VLM trends are explained by solid-earth deformation related to cryospheric and hydrological processes. In contrast, we note that for some regions, such as North America, the removal results in the appearance of substantial residual trends. A likely candidate for this residual trend is ~~the uncertain GIA contribution. Since we use a global model , which~~ unquantified uncertainty in the GIA term: the global model that we use does not account for lateral variations in the mantle viscosity structure and is not optimized for a specific region, ~~regional misfits may occur. Furthermore, local and regional VLM may find its origin in other processes than deformation driven by GIA and PDMR~~and uncertainties in the deglaciation history that are not fully represented in the GIA ensemble could lead to an underestimation of the uncertainty in formerly glaciated regions.

~~Because of PDMR-driven deformation,~~ VLM trends derived over the GNSS record length can be substantially affected by ~~PDMR~~ contemporary mass redistribution variability, which causes biases when these trends are extrapolated to explain VLM over longer tide-gauge records. This bias ~~could affect~~ affects global and regional sea-level reconstructions and projections that depend on VLM-corrected tide gauges. VLM ~~corrections~~ estimates derived from differences between satellite altimetry and tide-gauge observations (**??**) are also affected by this bias. Correcting tide-gauge observations with the ~~corrected~~ residual VLM trends instead of ~~original~~ observed VLM trends avoids this ~~bias.~~ source of bias. For a set of long tide-gauge records, correcting tide gauges ~~for the deformation-corrected GNSS~~ using the residual VLM trends not only results in a smaller spread between stations, but it also reduces the gap between the long-term trend at these stations and trends found in recent global-mean sea-level reconstructions that was found by **?**. Note that we have only applied our method to a limited subset of tide gauges, which means that the reduction in local sea-level trends and the spread among stations is not necessarily representative for other tide gauges. Whether correcting tide gauges using our method affects global sea-level reconstructions ~~. However, in this study we haven't fully separated the observed trends: many unmodelled processesremain in the data, and a~~ is therefore still an unanswered question.

This approach comes with multiple limitations. The GRACE solutions have a limited temporal and spatial resolution: since the observations only cover the period 2002-2017, GNSS observations from outside the GRACE period have been discarded, which, for some stations, substantially shortens the records, as displayed in Figure 5. This limitation means that the results of this study can be improved if SED estimates are expanded to cover the full GNSS record. Models of mass redistribution could be used for this purpose. While for ice mass changes model results show good agreements with observations, model estimates of TWS changes are still less reliable than GRACE observations (**?**), which in turn limits the ability to use models to estimate

SED. Due to the coarse spatial resolution of the GRACE data, sharp gradients in mass redistribution are smeared out over larger areas. Since SED is sensitive to these local mass changes, the SED computed here could under-estimate local SED in regions with strong spatial gradients. This issue could be one of the reasons of the un-explained residual land motion around Greenland, Antarctica, and Alaska visible in Figure 10c. Another limitation is that we compute SED with an elastic model that assumes a laterally uniform Earth structure. In some regions, such as West-Antarctica, elastic properties can deviate from their global-mean values and visco-elastic effects could occur on decadal time scales, which leads to additional deformation on top of the elastic response (e.g. **?**).

Another important limitation is that we only consider the effects of solid-earth deformation due to GIA and contemporary mass redistribution, while many other local and large-scale processes, such as tectonics and local subsidence due to groundwater and hydrocarbon extraction, are still present in the residual VLM time series. Like SED, many of these processes are also highly non-linear, and therefore also cause problems when records are extrapolated. Therefore, the linear trend in residual VLM that we have computed cannot be regarded as the secular background trend that is free from any bias when extrapolated back in time. A full understanding of these processes is key to fully understand the impact of vertical land motion on tide-gauge observations. We hope that the method presented here will serve as a base for future studies to further separate the observed VLM trends into individual components by integrating new models of physical processes~~, such as the deformation due to post-seismic relaxation, sediment compaction, and groundwater depletion.~~ .

*Data availability.* The GRACE estimates, deformation and RSL fields, and the observed and residual VLM trends can be downloaded from https://thomasfrederikse.stackstorage.com/s/HmjcG6n4mhmHTi4. The data and codes have been obtained from the following web sites: GNSS time series and MIDAS code: http://geodesy.unr.edu/. Tide-gauge observations: http://www.psmsl.org. ICE6G-D GIA model predictions: http://www.atmosp.physics.utoronto.ca/~peltier/data.php. Hector trend estimation software: http://segal.ubi.pt/hector/

*Author contributions.* TF and FWL conceived the idea for the study, TF and LC ran the computations, and all authors contributed to the manuscript.

*Competing interests.* The authors declare no competing interests

*Acknowledgements.* All figures have been made using the Generic Mapping Tools (GMT). This research was conducted at the Jet Propulsion Laboratory, which is operated for NASA under contract with the California Institute of Technology.